W-AM-Sym1 **NEURONAL INTEGRAL MEMBRANE PROTEINS**
Organized by Bertil Hille and Charles F. Stevens

Those of us interested in the special membrane proteins responsible for neuronal function find this an exciting time: the last five years have seen a revolution in our ability to study the function and structure of these proteins, and new information is increasing rapidly. The challenge of the coming years will be to relate structure to function, and this symposium focuses on some of the approaches we believe will pay off. How can we discover the three dimensional structure of membrane proteins? Nigel Unwin will tell us and at the same time describe the structure of the acetylcholine receptor channel. How can proteins be reconstituted and studied in defined systems? Chris Miller will explain the technique and illustrate it with two specific examples (a Cl channel and a Ca activated K channel). How are structure/function relationships to be investigated? Mary Jane Gething will describe the molecular biological approach of systematically altering protein structure and will illustrate it with studies on a system that may be the best model for the mechanism of vesicle membrane fusion during transmitter release. Given a protein's structure how can we make it come alive? Andy McCammon will describe the molecular dynamics approach to rate theoretical descriptions.

W-AM-Sym2 HIGH RESOLUTION STRUCTURE OF THE ACETYLCHOLINE RECEPTOR CHANNEL, Nigel Unwin

W-AM-Sym3 ANALYSIS OF THE STRUCTURE, FUNCTION AND INTRACELLULAR TRANSPORT OF AN INTEGRAL MEMBRANE PROTEIN - THE HAEMAGGLUTININ OF INFLUENZA VIRUS. M.-J. Gething, M. Roth, C. Doyle, S. Sharma and J. Sambrook. Cold Spring Harbor Laboratory, Cold Spring Harbor New York, N.Y.11724, U.S.A.

In recent years, we have used the haemagglutinin (HA) of influenza virus as a model to study eukaryotic integral membrane proteins. Our major interests are two-fold; firstly to correlate structure with function by identifying and analysing the protein domains or epitopes involved in receptor recognition, enzyme activity and antigenicity, and secondly to understand the mechanisms that determine the route of transport and final destination of nascent glycoproteins in eukaryotic cells. HA is the best characterized of all integral membrane proteins: its three-dimensional structure is known and the location of its major antigenic sites, the points at which it is glycosylated, its organization into trimeric structures and its orientation with respect to the membrane have been defined. Furthermore, the biosynthesis of HA utilizes host cell enzymes and processes for translation, membrane transport, glycosylation and maturation. The cloned gene for HA can be expressed with very high efficiency in mammalian cells, and the newly-synthesized HA is transported to the cell surface along a route similar, if not identical, to that believed to be taken by the majority of authentic cellular membrane proteins. The HA produced from the wild-type gene is displayed on the cell surface in a glycosylated form that is both biologically and antigenically active. It is therefore feasible to introduce mutations into the cloned HA nucleotide sequence, to express the altered genes in eukaryotic cells and to analyse the phenotype of the mutant proteins. Experiments will be described in which sequences encoding the three hydrophobic domains (the signal sequence, the fusion peptide and the transmembrane anchor) and the cytoplasmic tail of the HA molecule have been altered, deleted or exchanged for those of other eukaryotic membrane proteins.

W-AM-Sym4 GOING FISHING FOR ION CHANNELS.

Christopher Miller, Grad. Dept. of Biochemistry, Brandeis Univ., Waltham, MA 02254.

In this presentation I discuss the use of ion channel reconstitution as a strategy for the eventual isolation of channel proteins not amenable to conventional biochemical approaches. Two different channels will be employed as examples of the approach: the Cl^- channel of Torpedo electroplax, and the Ca^{++}-activated K^+ (CaK) channel of mammalian muscle. Each of the channels displays a rich variety of conduction and gating properties which make them attractive candidates for isolation. In the case of the Cl^- channel, I illustrate our struggles, unsuccessful as yet, to develop a suitable assay for purification, lending to lessons about the limitations of planar bilayer methods. The CaK channel provides an example of the power of the planar bilayer approach to identify, purify, and characterize toxins specifically directed against channel proteins. The use of charybdotoxin, a CaK-targeted protein toxin from scorpion venom, as a potential biochemical label of the CaK channel will be discussed.

W-AM-Sym5 DYNAMIC BEHAVIOR OF PROTEINS. J. Andrew McCammon, Department of Chemistry, University of Houston, Houston, Texas 77004.

Theoretical modeling of the structure and dynamics of biological molecules has developed rapidly and is becoming a useful tool in the interpretation of biological activity. This lecture will provide an introduction to several new methods that are likely to be helpful in the study of fundamental processes in neurochemistry. Among the methods to be discussed are ones that have allowed more detailed and realistic treatments of diffusional encounters between ligands and receptors,[1] solvation effects in ion-ion[2] and ion-receptor[3] interactions, and local conformational changes with long time scales in proteins.[4] This work has been supported by NSF (Biophysics Program and Office of Advanced Scientific Computing), NIH, the Robert A. Welch Foundation, the Alfred P. Sloan Foundation, and the Camille and Henry Dreyfus Foundation.

1. S.H. Northrup, S.A. Allison & J.A. McCammon, J. Chem. Phys. 80, 1517 (1984).
2. M. Berkowitz, O.A. Karim, J.A. McCammon & P.J. Rossky, Chem. Phys. Lett. 105, 577 (1984).
3. B.L. Tembe & J.A. McCammon, Comp. Chem., in press.
4. J.A. McCammon, Rep. Prog. Phys. 47, 1 (1984).

W-AM-A1 Current voltage relationship for the light driven proton pump bacteriorhodopsin. Gabor Szabo and Ernst Bamberg, Dept. of Physiology and Biophysics, University of Texas, Medical Branch, Galveston TX 77550 and Max-Planck-Institut für Biophysik, D 6000 Frankfurt 70, West-Germany.

Electrical properties of the photo-energized proton transport in purple membranes (PM) of Halobacterium Halobium, were investigated by measurements of the steady-state photocurrent under voltage-clamped conditions. Membranes were formed by depositing, in an oriented manner, fragments of purified PM onto a lipid bilayer support. The ion carriers FCCP and monensin were used to render permeable the lipid bilayer, which is fluid, without inducing ion transport in the PM, which is crystalline and therefore remains unaffected by mobile ion carriers. In the absence of illumination, electrical potentials applied across the membrane elicited negligibly small currents, indicating that the dark conductance of PM is low ($G_{dark} < 10\text{-}7$ S/cm^2). Illumination of PM increased its conductance. This increase is proportional to the light intensity, the proportionality coefficient being 1.21 S/watt for a thermal source of 3200°K. At high levels of illumination (I > 0.59 watts/cm^2) PM conductance ceased to increase with intensity, remaining constant near 4.6×10^{-5} S/cm^2.

Measurements of the photocurrent elicited by steady illumination for a large range of applied potentials ($\pm$ 150 mV) revealed a steep, nonlinear dependence of pump current on membrane potential. That even the largest (-150 mV) of the potentials applied against the photocurrent could only reduce but not reverse it, implies a pump reversal potential larger than 150 mV. These observations are in qualitative agreement with the predictions of barrier models for active ion transport. Supported by NIH Grant HL 24820 and the Max-Planck-Institut.

W-AM-A2 STRUCTURAL CHANGES IN BACTERIORHODOPSIN DURING THE M STATE ARE LIMITED IN NUMBER AND CONFINED TO HIGH RESOLUTION. R.M. Glaeser, Dept. of Biophysics, University of California Berkeley, CA 94702

High resolution electron diffraction data have been recorded for glucose-embedded purple membrane specimens in which bR has been trapped by slow cooling to below -100° C under continuous illumination. Thin films (O.D.~0.7) of glucose-embedded membranes, prepared as a control, show virtually 100 per cent conversion to the M state, and stacks of such thin film specimens give very similar x-ray diffraction patterns in the bR_{568} and the M_{412} state. Two independent sets of electron diffraction intensity differences were recorded for equatorial, i.e. (hko), reflections. There is little correlation for ΔF values at low resolution (20Å to 5.3Å, 51 reflections) but the correlation coefficient is about 0.3 at high resolution (5.3Å to 3.3Å, 221 reflections). The mean ΔF and the correlation coefficient can be used to estimate the true ΔF due to structural changes occurring in the M state. The magnitude of the mean ΔF is equal to what would be produced if eleven atoms were moved to structurally uncorrelated (i.e. new) positions in the M state, and furthermore these structural changes must leave the low resolution features (<5.3Å) essentially unchanged. Movements of a few, spatially well separated specific amino acid side chains with little or no movement of the α-carbon backbone, or a repositioning of atoms of the retinal group and the associated lysine side-chain following cis-trans isomerization are the two most probable causes of the observed intensity changes in the M state.

W-AM-A3 FEMTOSECOND SPECTROSCOPY OF BACTERIORHODOPSIN EXCITED STATE DYNAMICS. M. C. Downer, M. Islam*, C. V. Shank, AT & T Bell Laboratories, Holmdel, NJ 07733; A. Lewis, A. Harootunian, and Song Tan, Department of Applied Physics, Cornell University, Ithaca, NY 14853 (*Present Address Department Electrical Engineering, M. I. T., Cambridge, MA 02138).

We employ recent advances in femtosecond measurement techniques to study ultrafast photochemical changes in bacteriorhodopsin at physiological temperatures. A flowing sample of bacteriorhodopsin was used together with a pump and probe technique in order to obtain time resolved transmission spectra as photo-excited bacteriorhodopsin (bR_{570}) was created and decayed and as the primary photochemical product was created. To obtain these time resolved spectra between 570 and 620 nm, probe pulses of a 130 fsec white light continuum were used. The spectra show strong bleaching at 570 nm and increased absorption at 620 nm as a function of time from 0.2 to 5.0 psec. We find that the growth of the induced 620 nm absorption exactly fits the decay of excited bR_{570}. Both the excited bR_{570} decay and photochemical product production fit a single exponential with a time constant $\tau = 0.7 \pm 0.1$ psec in H_2O. Thus, we determine for the first time that the excited state of bacteriorhodopsin decays with the same time constant with which the ground state photochemical product is formed. In addition, we show that in D_2O the data also fit a single exponential with a time constant $\tau = 1.0 \pm 0.1$ psec. No deuteration dependent ground state processes are detected. Finally, our data demonstrate that the intensity of the excitation pulse can influence the dynamics of the absorption spectra.

W-AM-A4 ON THE RAPID FORMATION OF THE FIRST RED-SHIFTED GROUND-STATE PHOTOPRODUCT J IN THE PHOTOCYCLE OF BACTERIORHODOPSIN: ISOMERIZATION OF THE RETINAL MOLECULE OR PROTON MOVEMENT?
H.-J. Polland*, W. Zinth, M.A. Franz and W. Kaiser, Technische Universität München, D-8000 München, FRG, E. Kölling and D. Oesterhelt, MPI für Biochemie, D-8033 Martinsried, FRG, Intr. by E. Bäuerlein.

Concerning the primary process in bacteriorhodopsin conflicting data have been reported for the fluorescence life time and for the kinetics of the absorption changes.

Here we report on new experimental data obtaining a consistent picture of the primary events in bacteriorhodopsin. The improved experimental system has a time resolution of approximately 0.5ps and a low excitation level of only 0.1 absorbed photons per molecule. We find a red-shifted ground-state photoproduct J, which is formed in τ_1=0.7±0.3ps and which decays with τ_2=5±1ps. The same experiments with deuterated samples did not show changes in the time constants τ_1 and τ_2. Quite differently, with bacteriorhodopsin containing a sterically fixed retinal, we observe only the rapid build-up and a prolonged decay time of the excited singlet-state but no formation of a ground-state photoproduct. Our experimental results suggest the rapid isomerization of the retinal molecule in bacteriorhodopsin within τ_1=0.7±0.3ps.

*present adress at MPI für Festkörperphysik, D-7000 Stuttgart, FRG.

W-AM-A5 TWO KINETICALLY AND SPECTRALLY DISTINCT M INTERMEDIATES IN THE PHOTOCYCLE OF BACTERIORHODOPSIN.
M.K.Mathew, S.L.Helgerson, D.Bivin and W.Stoeckenius. Cardiovascular Research Institute and Department of Biochemistry and Biophysics, UCSF, San Francisco, CA 94143.

Bacteriorhodopsin is an electrogenic light-driven proton pump in the membrane of H. halobium. The kinetics of the bR photocycle are sensitive to membrane potential. Two kinetically distinct M-like intermediates have been reported in closed (vesicular) membrane systems - whose amplitudes depend on the membrane potential [1] - and in sheets [2]. Cell envelope vesicles suspended in 3M NaCl + 50 mM HEPES, pD 7.5 (in D_2O) and illuminated with 592 nm light have a difference peak for the faster decaying M_1 at 412 nm while the slower M_2 is centered at 405 nm. Each of these forms can be studied in de-ionized purple membrane sheets (blue membrane) which have been titrated back to purple with organometallic cations. Trimethyltin (TMT) and triphenyltin (TPT) reconstituted membranes have M-intermediates centered at 412 nm and 405 nm respectively. The TMT-membranes have a photocycle similar to that seen for native bR while TPT-membranes exhibit a much slower cycle.

The two kinetically resolved M forms are spectrally distinct species. Thus regulation of the electrogenic pumping efficiency of bR can be controlled if the two forms are on pathways with differing proton pumping stoichiometries. We propose that the branching event is regulated by an electrostatic interaction between the transmembrane electric field and a protein-cation binding site.

References: 1. Groma et al (1984) Biophys. J. 45:985-992.
2. Kuschmitz D and Hess B (1981) Biochemistry 20:5950-5957.
(Supported by NIH Program Project Grant GM-27057).

W-AM-A6 LINEAR POLYENES FORM PIGMENTS WITH BACTERIOOPSIN WHICH DO NOT PHOTOCYCLE OR PUMP PROTONS,
R. Crouch, J. Zingoni, C. H. Chang, R. Govindjee, and T. G. Ebrey, Medical University of South Carolina, Charleston, SC, and University of Illinois, Urbana, IL

Bacterioopsin pigment analogue studies have established that stable, functional pigments can be formed from retinal derivatives which do not contain the cyclohexyl ring. To investigate the retinal structure-pigment function relationship, we have prepared polyenes 1, 2 and 3 which approximate portions of the retinal side chain in order to determine a) if bacterioopsin pigments can be formed and b) if these pigments undergo a photocycle and pump protons.

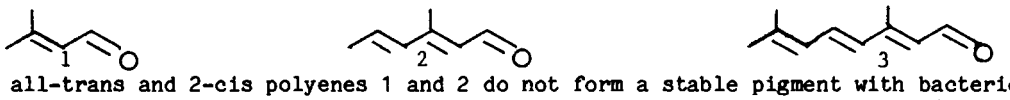

The all-trans and 2-cis polyenes 1 and 2 do not form a stable pigment with bacterioopsin. Both the all-trans and 2-cis polyene 3 do form pigments with bacterioopsin (λ max 422 and 420nm respectively). These pigments are slower to regenerate than bacteriorhodopsin. The polyene chromophore is displaced over 2 hours by either hydroxylamine or all-trans retinal indicating the interaction of the chromophore with the protein is not as strong as with retinal itself. On exposure to light there is a shift to 425 nm for both pigments. However, no M type intermediate or proton pumping is observed. The methylated polyenes, therefore, can interact with the binding site if the chain length is at least three ethylene units. However, structural requirements for the photocycling and proton pumping functions have not been fulfilled with these shortened chains.
(Supported by grants NIH EY04939, NSF PCM-01924, and DEA ER12087.)

W-AM-A7 NEUTRON DIFFRACTION STUDIES ON THE LOCATION OF RETINAL AND THE Ln-BINDING SITES IN BACTERIORHODOPSIN. F. Seiff, I. Wallat, and M.P. Heyn, Biophysics Group, Freie Universitat Berlin, Berlin, F.R.G.

Partially deuterated retinal, containing 10 deuterons in the polyene chain was incorporated in bacteriorhodopsin (bR) by adding it to the growth medium of a retinal-minus mutant. The in-plane neutron diffraction from oriented purple membranes (PM) from this sample and a similarly prepared sample containing protonated retinal was measured at the ILL in Grenoble. The Fourier difference map for the projected structure of bR shows that the labeled part of the retinal is in the interior of bR on the inside of helix 6. Upon deionization the PM turns blue (Kimura et al., in press). Addition of di - or trivalent cations restores the purple color suggesting that one of the cation binding sites might be close to the chromophore. Analysis of the binding data indicates that some binding occurs that is not accompanied by a color change (K-D. Kohl private communication). The binding sites for lanthanide ions are of particular interest since La is believed to inhibit the proton pump. Blue membranes were therefore regenerated with Dys 162 and Dys 164. The Fourier difference map for these 2 isomorphous samples at a 2:1 Dys/bR ratio shows two peaks, indicating that well-defined sites exist. These samples were further characterized by X-ray diffraction, flash photolysis and absorption spectroscopy. Further experiments at various Dys/bR ratios will be required to determine which site is occupied first, which one is responsible for the color change and which one is involved in the inhibition of the pump.

W-AM-A8 NEUTRON DIFFRACTION STUDIES OF RECONSTITUTED BACTERIORHODOPSIN

Jill Trewhella*, J.-L. Popot+, D.M. Engelman+, G. Zaccai#

*Los Alamos National Laboratory, Life Sciences Division, Los Alamos NM 87545
+Yale University, Dept.of Molecular Biophysics and Biochemistry, New Haven CT 06511
#Institut Laue-Langevin, 38042 Grenoble Cedex France

Bacteriorhodopsin molecules were reconstituted from the chymotryptic fragments described by Khorana et al[1]. The reconstituted molecules formed a p3 lattice in the presence of native lipids. X-ray and neutron diffraction data show intensity distributions and lattice spacings that are similar to native purple membranes. The reconstitution was done with both fragments fully hydrogenated, as well as with the smaller fragment (residues 1-71) fully deuterated and the larger fragment (residues 72-248) hydrogenated. Two dimensional neutron diffraction data were collected and a model building analysis, based on the known sequence[2] and the low resolution structure[3], has given the location of the deuterated portion of the molecule in the structural map.

[1]Huang et al. (1981) J. Biol. Chem., 256:3802-3809
[2]Ovchinnikov et al. (1979) FEBS Lett., 100:219-224; Khorana et al. (1979) PNAS, 76:5046-5050
[3]Henderson and Unwin (1975) Nature (London), 257:28-32

W-AM-A9 LIGHT-INDUCED REACTION OF BACTERIORHODOPSIN WITH N,N'-DICYCLOHEXYLCARBODIIMIDE (DCCD): LOCATION OF MODIFIED SITE. R. Renthal[1,2], M. Cothran[1], G. Espinoza[1], and K. Wall[2], U. of Texas at San Antonio[1], San Antonio, TX 78285, and U. of Texas Health Sci. Cntr.[2], San Antonio, TX 78284

Previous studies from this lab identified conditions for a light-induced reaction between the carboxyl-modifying reagent DCCD and bacteriorhodopsin (BR) in Triton X-100 micelles (BBRC 101:653, 1981). In Triton without DCCD, BR retains the photocycling and H^+ release/uptake properties of the H^+ pump. Thus, the site (or sites) modified by DCCD is likely to be involved in the proton pump mechanism. We have now further characterized the product of this reaction. [^{14}C]DCCD-modified BR (0.6 mol DCCD/mol BR) was cleaved with CNBr. The resulting peptides were purified by gel filtration and reverse phase HPLC. Three radioactive fractions were obtained. These peptides were completely absent in the absence of DCCD, and they were present only at low levels when DCCD was reacted with BR in the dark. All three had apparent molecular weights of 5200, as measured by dodecyl sulfate-urea gel electrophoresis. Both major [^{14}C]peptides, HC-2C and HC-2D, had amino acid compositions matching that expected for residues 69-118. HC-2C was partially cleaved with clostripain. The resulting mixture of residues 69-118 and 83-118 was subjected to automated sequence analysis. No evidence for intramolecular corsslinking induced by DCCD was observed. No significant amount of radioactivity was released with GLU 74 or ASP 85. Thus, the labeled site (or sites) is apparently at ASP 96, ASP 102, ASP 104 or ASP 115. These four carboxyl groups have been placed on the cytoplasmic half of the membrane in several structural models. Three possible roles of this site in the proton pump mechanism are: 1) involvement in H^+ uptake, 2) interaction with the β-ionone ring of retinal, or 3) exposure during a pump-linked conformational change. (Supported by grants from NIH)

W-AM-A10 STRUCTURE OF THE RETINAL CHROMOPHORE IN THE HR578 FORM OF HALORHODOPSIN.

S.O. Smith, M.J. Marvin and R.A. Mathies, Department of Chemistry, University of California, Berkeley, CA 94720, and R.A. Bogomolni, Cardiovascular Research Institute, University of California, San Francisco, CA 94143.

Halorhodopsin is a retinal-containing pigment that functions as a light-driven chloride ion pump in the cell membrane of Halobacterium halobium. To address the role of the retinal chromophore in chloride ion transport, resonance Raman spectra have been obtained of the hR578 intermediate of purified halorhodopsin using 514.5 nm laser excitation to maintain the pigment in the hR578 form. The close similarity of the frequencies and intensities of the hR578 Raman bands with those of light-adapted bacteriorhodopsin (bR568) shows that the chromophore in hR578 has a 13-trans configuration and that the protein environment around the chromophore in these two pigments is very similar. This suggests that hR578 experiences an electrostatic perturbation near the ionone ring similar to that identified in bacteriorhodopsin. We have shown that the configuration about the C=N bond can be determined by the sensitivity of the C_{14}-C_{15} stretching mode to N-deuteration [Smith et al. (1984) PNAS 81, 2055]. The 1204 cm^{-1} line in hR578 is assigned to the C_{14}-C_{15} stretch by comparison with bR568. This line shifts only 2 cm^{-1} to 1206 cm^{-1} in D_2O, demonstrating that hR578 has a C=N trans configuration. Furthermore, hR578 exhibits a Raman line at 1633 cm^{-1} which is assigned as the protonated Schiff base mode based on its shift to 1627 cm^{-1} in D_2O. The reduced frequency of the Schiff base stretching vibration compared with bR568 (1640 cm^{-1}) is shown to result from a reduction of its coupling with the NH in-plane rock. This may be due to a reduction in hydrogen bonding between the Schiff base proton and an electronegative counterion in halorhodopsin [Smith et al. (1984) J. Biol. Chem. 259, in press].

W-AM-A11 RHODOPSIN PHOTOREGULATES CAROTENOID AND RETINAL SYNTHESIS IN THE ALGA CHLAMYDOMONAS.

Foster, K.W.*, Saranak, J.*, Zarrilli, G.#, and Nakanishi, K.# *Physics Department, Syracuse University, Syracuse, N.Y. 13210; #Department of Chemistry, Columbia University, New York, N.Y. 10027.

Many plants, fungi, algae and bacteria have pigments which on light exposure cause induction of enzymes of the carotenoid synthesis pathway. On the basis of action spectra carotenoid-like, flavin-like and porphyrin-like pigments have been implicated. We have shown that a rhodopsin photoinduces carotenogenesis in Chlamydomonas reinhardtii. First, we found that the natural action spectra for induction was rhodopsin-like with a single peak at about 500 nm. The action spectra was obtained by taking advantage of the fact that in a mutant, FN68, carotenoid synthesis is required to make retinal and the threshold for phototaxis is an excellent measure of the amount made. This induction could be blocked by mRNA and protein synthesis inhibitors if given early enough. Second, we showed that incorporation of retinal analogs shifted the action spectrum compared to the natural pigment. 2 μM trans-7,8-dihydroretinal and 0.5 μM trans-3,4-dehydroretinal were added to occupy a small percentage of the available retinal sites. Respectively, blue shifted and red shifted action spectra were obtained for light induction of 500 nm-peaked-phototaxis sensitivity. This method could be used to determine the receptor in other species, other roles of rhodopsin, and the distribution of these roles in nature. Possibly eukaryotic rhodopsin originated as a regulator of carotenogenesis prior to its use in vision. Further, rhodopsin, a membrane receptor, can by its light activation control nuclear events; a possible role in all photoreceptor cells.

W-AM-B1 BUMETANIDE INHIBITION OF ANION EXCHANGE IN HUMAN RED BLOOD CELLS. R. B. Gunn, Department of Physiology, Emory University School of Medicine, Atlanta, GA 30322.

Bumetanide is commonly used as an inhibitor of Na,K,Cl cotransport systems, but this inhibition is not specific. ^{36}Chloride-chloride exchange was measured as tracer efflux at 0°C using a rapid filtration technique. The observed characteristics mimic many of those reported for the inhibition of Na,K,Cl cotransport in human red cells. Bumetanide was a mixed inhibitor at the external surface with K_I = 99 + 21 μM for the unloaded transporter and K'_I = 361 + 46 μM for the Cl-loaded transporter. A Hill plot had n = 0.987, consistent with a single inhibitor binding site. The inhibition was fully reversible either by washing the cells before loading with ^{36}Cl or by initiating the efflux of treated cells in bumetanide-free media. Preloading cells with bumetanide did not enhance the inhibition measured by having bumetanide only in the efflux solution. The percent inhibition of external bumetanide was independent of pH_{out} between 7.8 and 5.0. Na_o and K_o promote bumetanide inhibition of chloride flux relative to choline media. ATP depletion by 2 h incubation at 37°C in 10 mM inosine, 2 mM iodoacetate caused a 12% reduction in chloride flux. 10^{-4} M bumetanide reduced the flux of control cells 20% and ATP depleted cells 20% (30% from undepleted controls). cAMP and dibutryl cAMP did not enhance inhibition. The assumption that bumetanide is a specific inhibitor of Na,K,Cl cotransport processes is wrong in human red cells and is probably a dangerous assumption in most other cells. The use of radiolabeled bumetanide as a tag for the cotransporter may be improper in cells containing a band 3-like anion transporter. (Supported in part by NIH grants GM30754 and HL28674.)

W-AM-B2 HUMAN ERYTHROCYTE BAND 3 PROTEIN: AMINO GROUP MODIFICATION BY ACTIVE ESTER CROSS-LINKERS. M.L. Jennings, Dept. of Physiology & Biophysics, Univ. of Iowa, Iowa City, IA 52242.

BS^3 [bis(sulfosuccinimidyl)suberate] is a membrane-impermeant active ester that forms covalent inter- and intramolecular cross-links at the extracellular surface of band 3 in intact human red blood cells (Staros & Kakkad 1983. J. Memb. Biol. 74, 247). We have shown that the intermolecular cross-link has no detectable effect on anion transport or on covalent binding of H_2DIDS (4,4'-diisothiocyanodihydrostilbene-2,2'-disulfonate). The intramolecular cross-link, however, completely prevents covalent H_2DIDS binding. The intramolecular BS^3 cross-link is between the 17,000 dalton chymotryptic fragment and the 28,000 dalton C-terminal papain fragment, suggesting that BS^3 and H_2DIDS cross-link the same two lysine residues. Unlike H_2DIDS, the covalently bound suberate residue does not completely inhibit anion transport. This was shown by treating cells with BS^3 at pH 7.4, washing, and measuring the Cl-Br exchange flux (140mM Br_o) at intracellular pH 7 and extracellular pH between 4 and 10. At pH_o above 8, the flux is inhibited by more than 90%. Surprisingly, however, the flux in the treated cells is activated by lowering the extracellular pH below 8. At pH_o=6, the flux is almost as large as in control cells, although the apparent dissociation constant for Br_o is increased three-fold by the BS^3. At pH_o below 5, the anion flux in the BS^3-treated cells is inhibited by H^+, as in control cells. We interpret these results as evidence that neither of the modified amino groups is absolutely necessary for anion transport; the positive charge normally provided by the amino groups can be replaced by lowering the extracellular pH. The BS^3 treatment has also uncovered a second protonatable site of potential functional significance at the outer surface of band 3. Supported by NIH R01 GM 26861 and RCDA K04 AM 01137.

W-AM-B3 TARGET ANALYSIS STUDIES OF HUMAN RED CELL WATER AND UREA TRANSPORT. A.S. Verkman, J.A. Dix, C.Y. Jung and D.A. Ausiello. Division of Nephrology, University of California, San Francisco; State University of New York at Bighamton and Buffalo and Massachusetts General Hospital, Boston, MA.

Radiation inactivation was used to determine the nature and molecular weight (MW) of water and urea transporters in the red cell. Red cells were frozen to -50° C in a cryoprotectant solution, irradiated with 1.5 MeV electrons, thawed, washed, and assayed for osmotic water and urea permeability by stopped-flow light scattering. The freezing process did not affect the rates of water or urea transport, or the inhibitory potency of pCMBS on water transport and of phloretin on urea transport. Red cell urea transport inactivated with radiation (0-4 Mrad) with a single target size of 355 ± 20 kDaltons. 40 μM phloretin inhibited urea flux by ~50% at each radiation dose, indicating that urea transporters surviving radiation were inhibitable. Water transport did not inactivate with radiation (target size ~0.6 ± 12 kDaltons), and the inhibitory potency of 2.5 mM pCMBS decreased from 86 ± 1 % to 4 ± 9 % over a 0-2 Mrad dose range. These studies suggest that red cell water transport either requires one or more low MW proteins or is lipid mediated; there is a high MW pCMBS binding protein which regulates water flow. Red cell urea transport is mediated by a specific, high MW protein. These results do not support the hypothesis that band 3 (180 kDalton dimer) mediates red cell osmotic water and urea transport.

W-AM-B4 THE EFFECT OF CA AND CELL SHRINKAGE ON THE NA AND K PERMEABILITY OF THE HUMAN RED BLOOD CELL MEMBRANE. Lynn M. Crespo, Terri S. Novak and Jeffrey C. Freedman, Depts. of Pharmacology and Physiology, State University of New York, Upstate Medical Center, Syracuse, NY 13210.

In normal human red blood cells, the intracellular concentration of free calcium, or Ca_c, is closely regulated and maintained at submicromolar levels. When Ca_c increases above 1μM there is a specific increase in the K permeability of the membrane (Gárdos effect) resulting in rapid K loss and cell shrinkage. In order to examine possible effects of Ca_c on Na permeability, fresh washed cells were incubated in (mM) 140 NaCl, 5 KCl, 10 Hepes, 5 glucose, 0.12 $MgCl_2$, $2Na_2HPO_4$, 0.025 EGTA, pH 7.4 AT 37°C with 2μM calcium ionophore A23187 and 0.03μM to 1.0mM external free Ca, or Ca_o. At greater than 3μM Ca_o the cells gained 48±13 μmoles Na/gHb (SD, n=20) in 3 hours as ATP fell to less than 10% of normal. The net gain of Na is prevented by EGTA and independent of [A23187] between 0.3 and 3.0μM. The same Na gain is obtained in cells in which ATP depletion is inhibited by 0.5 mM Na-orthovanadate. An equivalent amount of Na is gained in 3 hours by ouabain treated cells exposed to 1μM valinomycin, or by cells shrunken by the addition of sucrose to 0.5M. In addition to gaining Na, the cells shrunken in sucrose lose 27% of their K contents. When the cells which had been treated with Ca + A23187 or sucrose for 3 hours are subsequently transferred to a Na free, high K medium, the Na and K contents which had changed slowly over 3 hours are now restored to normal within 10 minutes, suggesting that a fraction of cells has become highly permeable to Na and K. These observations suggest that prolonged shrinkage induces a subpopoulation of cells to become highly permeable to Na and K, and that the effect of Ca_c on the Na permeability of the human red blood cell is an indirect consequence of cell shrinkage due to K loss. Supported by USPHS grant 1R01GM28839 and by a grant-in-aid from the AHA/Upstate NY Chapter.

W-AM-B5 THE MECHANISM OF HEMOLYSIS OF SICKLE RED BLOOD CELLS. Kurumi Y. Horiuchi, Kazumi Horiuchi and S. Tsuyoshi Ohnishi, Dept. of Hematology and Medical Oncology, Hahnemann University School of Medicine, Phila., PA

It is well known that the anemic condition of sickle-cell patients is caused by an accelerated hemolysis of red blood cells. Serjeant et al. demonstrated a significant correlation between the percentage of irreversibly sickled cells(ISC) in the circulation and the red cell survival (1). Recently, we developed a method to prepare ISC in vitro by exposing sickle red cells to repeated cycle of deoxygenation and oxygenation(2). Using this method, we investigated the mechanism of hemolysis of sickle red cells. We have observed the followings: (A) During 20 hours of the oxygenation-deoxygenation incubation, 15 % of sickle cells hemolyzed, while 3% hemolysis occured in normal cells; (B) During 20 hours of an oxygenated incubation, hemolysis of sickle cells was 5 %; (C)When sickle cells were separated according to the density(by a density gradient centrifugation), heavier cells (which consist of ISC) are more liable to hemolysis than lighter cells; (D)The percentage of hemolysis increased with an increase of calcium concentration in the incubation medium. The enhancing effect of calcium was more pronounced in the heavier cells; (E)Certain drugs demonstrated a protective action against the hemolysis.

References: (1)Brit. J. Haematol. 17:527(1969); (2)Brit. J. Haematol. 55:665(1983)

W-AM-B6 SICKLE CELL ANEMIA: A NEW MULTIPARAMETER BIOPHYSICAL CHARACTERIZATION

H.C. Mel, G.V. Richieri, Department of Biophysics and Medical Physics, University of California, Berkeley 94720, and D.T.Y. Chiu and B.H. Lubin, Children's Hospital Medical Center, Oakland, California 94609

The results of an initial phase of a new kind of systematic study of the cells of sickle cell anemia are presented. Normal and sickle (SS) cells have been analyzed in suspension, using the biophysical methodology of resistive pulse spectroscopy, under conditions that produce a coherent data-set of 9 cellular properties. The characteristics measured are of three types: Familiar, commonly-measured properties (e.g. modal and mean cell volume and volume distribution); familiar properties measured by new and different means (e.g. osmotic fragility, deformability, and mean surface area); and novel properties not generally measured by any means (e.g. cytoplasmic resistivity). Unique to this approach is that, for each individual, the full array of cellular properties is obtained from a single small sample of blood, in a short time frame. The matrix of all individual results, from the normal and SS patients, reveal both similarities and differences between individual and grouped properties. The data are analyzed in terms of (potential) underlying natural linkages between different cellular and subcellular properties. Guided by these model-interrelationships, a dimensionless, characterizing, multiparameter index is introduced which completely separates the control and SS samples into nonoverlapping classes.

W-AM-B7 EQUILIBRIUM POSITIONS AND STOICHIOMETRY OF THE FUROSEMIDE-SENSITIVE Na AND K FLUXES IN HUMAN RED CELLS WITH HIGH Na CONTENT. Carlo Brugnara, Mitzy Canessa, Daniele Cusi and Daniel C. Tosteson. Dept. of Physiology and Biophysics, Harvard Medical School, Boston, MA 02115.

We have previously shown (Biophys. J. 45:162a,1984), that when human red cells (RC) with high K content are incubated in a high Na medium (120 mM), the measured stoichiometry at the equilibrium position of the furosemide-sensitive (FS) Na and K fluxes was 2Na : 3K. We have measured FS ^{22}Na and ^{42}K efflux and influx, in cells with high Na and low K content (90-70 and 0-20 mmol/l cell, respectively). The flux media contained (mM) 120 NaCl, 0-30 KCl, 1 $MgCl_2$, 10 TRIS-MOPS, pH 7.4 at 37°C, 10 glucose, 0.1 ouabain, with and without 1 mM furosemide. In the range of internal Na and K contents studied, at external K (K_o)=0, FS Na efflux was higher than FS Na influx. Therefore, in the absence of K_o, net FS Na and K efflux was observed. When K_o was increased, FS Na and K fluxes were both stimulated. However, the stimulation by K_o of the FS Na and K influx was greater than that of the FS Na and K efflux. Thus, the net FS Na and K extrusion was abolished by the increase in K_o. The concentration of K_o required to bring FS Na and K fluxes to equilibrium (efflux=influx) was a function of cell K content, and it increased when cell K was increased from 1 to 30 mM. At the equilibrium position of FS Na and K fluxes, the measured stoichiometry was 3Na : 2(1)K. Therefore, the stoichiometry of the FS Na and K fluxes is a function of the Na and K concentration ratios on both sides of the membrane. In 120 mM NaCl, 0-30 mM KCl media, the stoichiometry of the FS Na and K fluxes at the equilibrium position is 2Na:3K when K is the main internal cation, and 3Na:2(1)K when Na is the main internal cation.

W-AM-B8 TEMPERATURE DEPENDENCE OF STILBENE BINDING TO BAND 3 IN HUMAN RED CELL MEMBRANES. Richard G. Posner and James A. Dix, Department of Chemistry, SUNY, Binghamton, NY 13001

The binding characteristics of the inhibitor of anion transport in human red cells, 4,4'-dibenzamido-2,2'-disulfonic stilbene (DBDS), to band 3 in ghost membranes suspended in 150 mM NaCl, 5 mM HEPES, pH 7.4, have been measured over the temperature range 0-30 °C by equilibrium and stopped-flow fluorescence methods. The DBDS equilibrium dissociation constant, K, increased with temperature; no evidence of a "break" a log K vs 1/T plot was found. Stopped-flow kinetic studies resolve the overall binding into a bimolecular step followed by a unimolecular step; forward and reverse rate constants for each of the two steps can be determined from analysis of stopped-flow kinetic traces. Arrhenius plots of the rate constant data did not reveal any breaks. Arrhenius activation energies for the individual steps in the binding mechanism are (in kcal/mol) 11.6 ± 0.9 (forward, bimolecular), 17.4 ± 1.8 (reverse, bimolecular), 6.3 ± 2.3 (forward, unimolecular) and 10.6 ± 1.9 (reverse, unimolecular). These results suggest that there is an appreciable energy barrier for the bimolecular association of DBDS with band 3. If stopped-flow data is analyzed in terms of a single rate determining step, rather than two coupled binding steps, then an Arrhenius plot of rate data gives a break in the temperature range 12-19 °C, similar to reported red cell membrane transition temperatures determined by other methods. Supported by HL29488.

W-AM-B9 PHORBOL ESTER-INDUCED ALKALI METAL/H EXCHANGE IN AMPHIUMA RED BLOOD CELLS. Peter M. Cala, Dept. of Human Physiology, University of California, Davis, CA 95616

The Amphiuma red blood cell exhibits volume-sensitive alkali metal ion fluxes which function to return cell volume to normal levels following osmotic perturbation. When osmotically swollen a K/H exchange pathway is activated resulting in net K and volume loss. In contrast cell shrinkage activates a Na/H exchange which mediates cellular Na and therefore H_2O uptake. Previous studies have shown that increased intracellular Ca can stimulate K/H exchange yet the extent of stimulation by Ca was less than that in response to volume perturbation alone. Since intracellular Ca and protein kinase-C can act synergistically to produce a full physiological response, it was hypothesized that the protein kinase-C is important in activation of K/H exchange. Induction of protein kinase-C, by exposure of Amphiuma red blood cells to phorbol ester (12,13 didecanoate; PMA), produced a profound stimulation of alkali metal/H exchange. Unlike osmotic perturbation, which activates either K/H or Na/H exchange, PMA activates robust net Na and K flux pathways simultaneously. Based upon force flow analysis it was determined that the phorbol ester induced net Na and K fluxes represent Na/H and K/H exchange, respectively. The PMA-induced K/H exchange has characteristics normally associated with Na/H exchange (i.e. amiloride sensitivity) and the Na/H exchange exhibits behavior normally characteristic of K/H exchange (i.e. stimulation by Ca). Thus, it appears that if diacylglycerol, through protein kinase-C, is involved in activation of alkali metal/H exchange, in response to changes in Amphiuma red cell volume, then other events associated with cell swelling and shrinkage are responsible for determining K and Na selectivity. This work was supported by NIH grant HL21179.

W-AM-B10 EFFECTS OF N-ETHYLMALEIMIDE (NEM) ON OUABAIN-RESISTANT CATION FLUXES IN HUMAN RED CELL (RBC) GHOSTS. Deborah K. Smith and Peter K. Lauf (Intr. by B. Herman) Dept. Physiol., Duke Univ. Med. Ctr., Durham, NC 27710.

Human RBC membranes possess several transport pathways for monovalent ions, including a $K^+ + Cl^-$ cotransport recently described by us which is activated by NEM. We examined the properties of Rb^+ efflux from resealed ghosts in the absence and presence of 1 mM NEM. Rb^+-loaded ghosts were prepared by hypotonic lysis of RBC and subsequent resealing in the presence of 145 mM RbCl, 0.1 mM EGTA, and 0.1 mM ouabain. Washed resealed ghosts (at 1% v/v suspension) were incubated at 37°C in isotonic $NaNO_3$ or NaCl buffers containing EGTA and ouabain. Base level Rb^+ efflux occurred with a rate constant of $^{o}k_{Rb} = 0.48\ hr^{-1}$. However, in the presence of 1 mM NEM, there was a strong (~25-fold) stimulation of efflux into $NaNO_3$ ($^{o}k_{Rb} = 12\ hr^{-1}$) and a moderate (~6-fold) stimulation of efflux into NaCl ($^{o}k_{Rb} = 2.7\ hr^{-1}$). Such stimulation of efflux was observed in the presence of ≥0.2 mM NEM and increased at pH values approaching 8.0, consistent with titration of an SH group. When NEM-stimulated efflux rates were measured as a function of initial internal ghost Rb^+ concentration (~10-130 mM) using glucamine as replacement cation, Rb^+ efflux rates into NaCl tended to reach a maximum, while efflux rates in $NaNO_3$ increased further and more linearly, as has been reported for the Gardos effect of Ca^{++} activation of K^+ flux. Replacement of external Na^+ with glucamine or choline under standard flux conditions resulted in a decrease in NEM-stimulated Rb^+ efflux, suggesting a role for external Na^+. Further studies are in progress to examine in ghosts the possible relationship between NEM-stimulated Rb^+ efflux (which occurs in the absence of Ca^{++}) and the Ca^{++}-activated K^+ (Gardos) channel. (Supp. by NIH AM28236)

W-AM-B11 CYANINE DYE FLUORESCENCE USED TO MONITOR ELECTROCHEMICAL CHANGES IN MEMBRANES DURING INSERTION OF COMPLEMENT PROTEINS C5b-9. Therese Wiedmer and Peter J. Sims, Depts. of Pathology and Biochemistry, University of Virginia, Charlottesville, VA 22908.

The fluorescent potentiometric indicator diS-C_3-(5) has been used to study changes in membrane potential due to assembly of the C5b-9 membrane attack complex of the complement system. Human red blood cells and resealed erythrocyte ghosts bearing membrane-assembled C5b67 complexes (EAC1-7) were generated by immune activation in C8-deficient human serum. The membrane potential of EAC1-7 red cells and ghosts was unchanged from control red cells (-7 mV) and ghosts (0 mV), respectively. Addition of complement proteins C8 and C9 to EAC1-7 red cells resulted in a dose-dependent depolarization of membrane potential which preceded hemolysis. This prelytic depolarization of membrane potential -- and the consequent onset of hemolysis -- was accelerated by raising external $[K^+]$, suggesting that the diffusional equilibration of transmembrane cation gradients is rate-limiting to the cytolytic event. In the case of EAC1-7 resealed ghosts, no change in membrane potential could be detected after C8/C9 additions. When the membrane potential of the EAC1-7 ghost was displaced from O mV with valinomycin, a dose-dependent depolarization of the membrane was observed upon addition of C8 and C9. Lytic breakdown of the ghost membranes was <5%. Conclusions derived from this study are: (i) measured prelytic depolarization of the red cell Donnan potential confirms the colloid-osmotic theory of immune cytolysis (ii) diffusional transmembrane equilibration of Na^+ and K^+ through the C5b-9 pore is not electrogenic, but does appear to be rate-limiting to cytolytic rupture of the target erythrocyte (iii) carbocyanine dye fluorescent indicators can be used to monitor electrochemical changes arising from immune damage to the plasma membrane under both cytolytic and non-cytolytic conditions. (Supported by a Grant-In-Aid from the American Heart Association and the Jeffress Trust. PJS is a John A. Hartford Fellow).

W-AM-B12 EVIDENCE FOR BIVALENT CATION (Me^{2+}) INTERACTION WITH A H^+-SENSITIVE SITE ON THE OUABAIN-RESISTANT(OR) K^+Cl^- TRANSPORTER IN LOW K^+(LK)SHEEP RED CELLS. P.K.Lauf,Dept.Physiol.Duke Univ.Durham.

The effect of Me^{2+} and the cationophore A23187 was studied on OR Cl^--dependent $K^+(K^+Cl^-)$flux in LK sheep red cells (SRC). A23187 + EGTA(ethylene-glycol-tetracetic acid) stimulated OR K^+Cl^-flux severalfold in swollen or shrunken LK SRC but not in SRC treated with N-ethylmaleimide(NEM) or in high K^+ SRC lacking K^+Cl^- transport. Ca^{2+} concentrations up to 10^{-3}M in presence of A23187 inhibited OR K^+Cl^- flux stimulated by the ionophore, NEM or swelling. Effects were reversible and did not alter cell ATP. However, A23187 did not stimulate OR K^+Cl^- flux in ATP depleted SRC,an effect reversible upon metabolic repletion. Hence A23187+EGTA activated reversibly and to similar magnitude volume-sensitive K^+Cl^- flux stimulated,however, irreversibly by NEM. The activation may be explained by an equilibrium between free intracellular Me^{2+} and accumulated A23187 since, with transport of the ionophore-Me^{2+} complex not being rate limiting, the following Me^{2+} sequence of decreasing potency was found: $Mn^{2+} > Ca^{2+} > Mg^{2+} > Sr^{2+}$ with Ba^{2+} being ineffective. A second equilibrium exists between the free Me^{2+}_i and the K^+Cl^- transporter. It is proposed that cell swelling reversibly and thiol alkylation irreversibly cause debinding of Me^{2+} from and hence activate the K^+Cl^- transporter. Since after thiol alkylation A23187 + EGTA were ineffective to further stimulate K^+Cl^-flux, the putative Me^{2+} binding site may be controlled by an SH group that forms a thiolate-imidazolium or -lysine ion pair in the low but not in the high affinity binding state for Me^{2+}. By virtue of its H^+ titrability the site senses cellular H^+ and associated cell volume changes, while through modulation of its Me^{2+}-binding site affinity it regulates the activity of K^+Cl^- transport. Inhibition by A23187 + Me^{2+} requires presence of additional sites on the transporter or another molecule. Supp.by NIH grant AM 28236.

W-AM-C1 A MICROSCOPIC MECHANISM FOR THE NMR RELAXATION TIMES OF WATER IN BIOLOGICAL SYSTEMS.
C.F. Hazlewood, Baylor College of Medicine, Houston, Texas and H.E. Rorschach, Rice University, Houston, Texas.

The NMR properties of water in biological tissues have been intensively studied, yet the basic relaxation mechanism has remained elusive. Specifically the relaxation rate T_1^{-1} for water in most biological tissues and polymer solutions is characterized by a weak frequency dependence which is well-fitted by the equation (1): $T_1^{-1} = A\,\omega^{-\frac{1}{2}} + B$.

It is possible by superposition of two or more assumed fractions of water with differing correlation times to obtain $T_1(\omega)$ values that approximate equation (1) over a limited frequency range, but such models have generally been ad-hoc and provide little basic understanding of the relaxation mechanism. We propose a mechanism for the water-protein interaction that involves the wave-length-dependent correlation time for the fluctuations of the highly-damped excitation modes of a long flexible chain polymer. This leads to equation (1) in a natural way without the introduction of assumptions of water fractions with arbitrary distributions of correlation times.

W-AM-C2 NUCLEAR MAGNETIC RESONANCE SPIN ECHOES IN HYDRATED LYSOZYME
I.C. Baianu[+], T.S. Lioutas and M.P.Steinberg, Department of Food Science, University of Illinois at Urbana, [+]Physical Chemistry Laboratory, 1302 W.Pennsylvania Avenue, Urbana, Illinois 61801.

Proton NMR spin echoes were observed at 360 MHz for a wide range of lysozyme samples both in the solid state and in solution. The Ostroff-Waugh (OW) pulse sequence (1) was employed for studying lysozyme powders,while the Carr-Purcell-Meiboom-Gill (CPMG) sequence was used to determine the transverse relaxation time,T_2. Proton NMR spin echo spectra of hydrated lysozyme were computed as prescribed in ref.(2), in order to resolve the contributing proton populations. In agreement with previous work at low field (3), we find that a major population of water protons are in fast exchange with exchangeable lysozyme protons and with a major fraction of the water protons located in the hydration shell(s) of lysozyme. The transverse relaxation rate, R_2, of the slowest relaxing component - which relates to this fast exchange process- has a markedly non-linear dependence on lysozyme concentration. Diffusion barriers also appear to have little effect on the OW,spin echo half-height linewidths for hydrated lysozyme powders, and cannot, therefore, explain the observed non-linear dependence on lysozyme concentration. ^2H and ^{17}O NMR observations on hydrated lysozyme powders (4) and solutions (5), strongly correlate with our high-field proton NMR spin echo studies, and permit the determination of ^2H and ^{17}O correlation times for water in the hydration shells of lysozyme.

REFERENCES CITED:
1. Ostroff,S. and Waugh,J.S.(1966). Phys. Rev. Letts.,16(24),1097-1098; 2. Vold,R.(1978).In "Progr. NMR Spectr.",12, 79-133; 3. Hsi,E.et al.(1976).J.Phys.Chem,80,412-416; 4. Baianu,I.C.& T.Lioutas, (1984) Unpublished results; 5. Halle,B. et al.(1981). J.Amer. Chem.Soc.,103,500-508.

W-AM-C3 CONFORMATION OF BLOOD GROUP ACTIVE OLIGOSACCHARIDES ISOLATED FROM OVARIAN CYST MUCINS.
B. N. Narasinga Rao and C. Allen Bush, Department of Chemistry, Illinois Institute of Technology, Chicago, Illinois 60616.

The conformations of a series of H-active oligosaccharides, 3 to 6 residues long and terminating in N-Acetyl-galactosaminitol, have been studied by ^1H NMR spectroscopy. Both tri-and tetrasaccharide alditols exhibit positive n.O.e. at room temperature. For a pentasaccharide, in which the room temperature n.O.e. were very small, measurements were done at 70°C to take advantage of the dependence of rotational correlation time on temperature. The hexasaccharide alditol which showed no n.O.e. at 24°C, exhibited negative n.O.e. at 5°C and positive effects at 70°C. In the H-active type I sequence, shielding of fucose H3 is observed relative to that in type II structures because of interaction with the GlcNAc amide group. The reciprocal effect on the environment of GlcNAc amide is observed in the circular dichroism spectrum in the 200 nm region. Possible conformations obtained for type I and type II sequences by incorporating distance constraints derived from n.O.e data in the empirical energy calculations are found to have low energy values. In the third type of sequence, Fuc α-(1→2)-Gal-β-(1→3)-GalNAcol, the chemical shifts of fucose H3 and H4 are different from those in type I and type II. Close chemical shift correlations are observed for each of these sequences in structurally related oligosaccharides. There is very little temperature dependence of the chemical shifts or interring proton distances suggesting that the conformations are fairly rigid.

W-AM-C4 NMR STUDIES OF POLY d(G-T)·d(C-A) AND POLY d(A-T) AT HIGH AND LOW SALT. Bruce Jenkins and James L. Alderfer Biophysics Dept. R.P.M.I. Buffalo,N.Y. 14263
P-31 and H-1 NMR spectra have been obtained for poly d(G-T)·d(C-A) as a function of both temperature and salt. The P-31 spectrum of poly d(G-T)·d(C-A) is a quadruplet at high CsCl or high temp. At low salt the spectrum is an unresolved quadruplet. H-1 NMR assignments have been made at high and low temperature of all the base and H-1' protons. The exchangeable T(H-3) and G(H-1) protons occur at 13.3 and 12.4 ppm at 30°C. In addition 1-D nOe difference spectra are reported for this polymer at low salt. NOe enhancements between H-8 protons of the purines and the respective H-5 protons of the pyrimidines (H and CH_3) and between the H-8,6 protons and the H-2',2" protons indicate a B-type conformation for this polymer. At high Cs^+ concentrations there are upfield shifts for A,C, and T (H-1') protons and A(H-2), but not G(H-1'). H-1 NMR measurements are reported for poly d(A-T) at low and high CsCl. Upon going to high CsCl there are selective upfield shifts for various protons, with the most dramatic being for T(H-1'). A(H-8) does not shift downfield as observed in CsF. NOe measurements indicate that at high Cs^+ the polymer is in a B-type form similar to that at low salt. Assignments and nOe effects at low salt agree very closely with those of Assa-Munt and Kearns (Biochem. 23, 1984 791) indicating a B-type helix. At high temperatures some of these protons undergo severe changes in linewidths. Those protons which undergo the largest upfield shifts upon binding Cs^+ also undergo the most dramatic changes in linewidths. In particular T(H-1'),T(CH_3), A(H-1'), and T,A(H-6,2) all undergo large changes in linewidths while A(H-8) and all the H-2',2" protons do not. The maximum linewidths all occur at 65°C indicating a temperature induced equilibrium between d.s. and s.s. DNA and bound and unbound Cs^+.

W-AM-C5 **MOLECULAR CONFORMATIONAL STUDIES OF HUMAN ERYTHROCYTE SPECTRIN USING ^1H - NMR SPECTROSCOPY** **H.-Z. Lu[1], W. P. Conway[1], J. Lupori[1], M. E. Johnson[2] and L. W.-M. Fung[1], [1]Department of Chemistry, Loyola University of Chicago, Chicago, IL 60626, and [2]Department of Medicinal Chemistry and Pharmacognosy, University of Illinois at Chicago, Chicago, IL 60680**

We have extracted the spectrin network from human erythrocyte membranes by low ionic strength buffer at 37C, and have further purified it by gel filtration at 4C to give two distinct bands on SDS polyacrylamide gel. Proton NMR at 200 MHz has been used to study spectrin as a function of temperature, ionic strength and spectrin concentration in deuterated phosphate buffer. The concentrations of the samples are in the mg/ml range. Several relatively sharp resonances on top of the broad envelope are observed in both the aliphatic and aromatic regions of the spectra, indicating the presence of relatively flexible local (side chain) motion or segmental motion of the molecule. The intensities of the resonances appear to be temperature and ionic strength dependent. For example, temperature studies of spectrin in 5 mM phosphate buffer at pH 7.4 suggest the existence of more local/segmental motion in the spectrin molecule at higher temperatures. We interpret the change in intensities as being due to changes in conformation and/or the association state (oligomers, tetramers and dimers) of spectrin. We have used non-denaturing polyacrylamide gel electrophoresis to follow the association states of our NMR samples in order to understand these local/segmental motions in spectrin molecules at relatively high concentrations.

Supported in part by grants from NIH (HL-01190 , HL-31145 and HL-23697)

W-AM-C6 ^{13}C CARBONYL CHEMICAL SHIFT TENSORS OF THREE GLYCINE DIPEPTIDES. Terrence G. Oas, T.J. McMahon, and F.W. Dahlquist, Institute of Molecular Biology, Univ. of Oregon, Eugene, OR 97403 and Gary Drobny, Department of Chemistry, Univ. of Washington, Seattle, WA 98195.

We have determined the glycine carbonyl ^{13}C chemical shift tensors of three dipeptides of the form N-acetylglycyl-X-amide, where X is alanine, tyrosine and phenyalanine. The tensors were determined from powders of the peptides labeled with ^{13}C at the glycine carbonyl and with ^{15}N at the amide nitrogen of the X residue. The resulting ^{13}C-^{15}N dipole coupled carbon chemical shift powder patterns allowed the determination of both the principal values as well as the molecular orientation of the shift tensors. The σ_{33} axis is presumed to be perpendicular to the peptide plane, based on previous single crystal studies and symmetry considerations. The orientation of the σ_{11} and σ_{22} axes in the peptide plane are determined by a single angle, derived from simulations of the $^{13}C/^{15}N$ dipolar coupled powder patterns. There is a significant difference in the σ_{22} value for glycyltyrosine, when compared with those of glycylalanine and glycylphenylalanine. This is in contrast to the chemical shift in solution, which is identical for all three. A cannonical shift tensor cannot be assumed for all peptide bonds and there is a significant effect of the crystal lattice on both the size and orientation of ^{13}C carbonyl shift tensors in peptides.

Dipeptide (Ac-glycyl-X-NH_2)	Glycyl Carbonyl Chemical Shift Tensor Principal Values (in ppm relative to external liquid benzene)			Angle between σ_{11} and C-N bond
X	σ_{11}	σ_{22}	σ_{33}	
Alanine	-120 ± 3	-60 ± 1	36 ± 3	35° ± 3
Tyrosine	-118 ± 3	-38 ± 1	35 ± 3	42° ± 3
Phenylalanine	-120 ± 3	-58 ± 2	36 ± 3	35° ± 3

W-AM-C7 BACTERIAL LUCIFERASE: A ^{13}C-NMR INVESTIGATION. J. Vervoort*, M. Ahmad, D. J. O'Kane, F. Muller*, and J. Lee, Departments of Biochemistry, *Agricultural University, Wageningen, The Netherlands, and University of Georgia, Athens, GA, USA.

Chemical shifts of ^{13}C-enriched FMN bound to Vibrio harveyi luciferase indicate extensive H-bonding in both oxidized and reduced states. Both states have a strong H-bond at the C(2) carbonyl, and one not as strong as compared to water, at the C(4) carbonyl. For bound FMN the C(10a) resonance has a strong upfield shift, i.e. a higher π-electron density on this atom, and the C(2) a slight upfield shift, both a result of H-bonding to N(1). Especially an upfield shift of the C(8) resonance allows us to conclude that the electron distribution of the polarized FMN here differs from that in flavodoxin. For luciferase bound reduced flavin the chemical shifts suggest that it has a planar configuration and also, from the C(2) and C(10a) shifts, that it is bound as the anion, $FMNH^-$, over the pH range studied, 7.0-8.5. Another important feature of the bound $FMNH^-$ spectrum is a downfield shift of the C(4a) resonance, indicating a decreased π-electron density on this atom. This shift is not affected by addition of dodecanal or dodecanol, so these substrates have no interaction at the C(4a) center in the reduced complex. Several of the benzene atoms show enhanced π-electron density. Some of the resonances show clear doublet character, interpreted as due to two non-identical binding sites for $FMNH^-$ on luciferase, one strong and the possible second much weaker. Flavin is bound similarly to other types of luciferases (Photobacterium phosphoreum and V. fischeri) so the observed differences in bioluminescence properties are probably not due to different electronic structure of the bound flavin. Work supported by SON/ZWO, NSF, and NATO.

W-AM-C8 CTPO SPIN LABEL AS A PROBE TO MEASURE BINDING OF TRANSITION METAL IONS TO MACROMOLECULES. W. Froncisz*, Ching-San Lai and James S. Hyde. National Biomedical ESR Center, The Medical College of Wisconsin, Milwaukee, Wisconsin. *On leave from the Jagiellonian University, Krakow, Poland.

It has previously been reported that collision of nitroxide free radicals with transition metal ions in a solution of low viscosity leads to changes in the spin label transverse and longitudinal relaxation probabilities. These changes can be observed as line broadening and altered saturation characteristics in CW ESR experiments (1,2). This phenomenom was utilized to study interaction of metal ions with proteins and phospholipid vesicles (3). Their approach, however, required rather high concentrations of metal ions (1-100 mM). In our studies of the use of the spin label CTPO as a probe to determine the concentration of dissolved oxygen in solution, the so-called K-parameter, which parameterizes the degree of resolution of couplings to protons of the spin label, was measured over a wide range of conditions. Based on this experience, we have found that the K-parameter of CTPO spin label is also very sensitive to the presence of transition metal ions. Using this parameter, one can study the concentration of paramagnetic metal ions in the range of 10μM to 1mM. It has been found that an analytical expression of the form $K = a + b\,[Me^{n+}] + c\,[Me^{n+}]^2$ describes the K-parameter as a function of metal ion concentration $[Me^{n+}]$ with a correlation better than 0.99. Using this method, the binding of Ni^{2+} and Cu^{2+} ions to a synthetic melanin polymer as a function of pH was studied.

1. K. M. Salikhov, A. B. Doctorov and Yn. M. Molin (1971), J. Mag. Reson. 5, 189-205.
2. J. S. Hyde and T. Sarna (1978), J. Chem. Phys. 68, 4439-4447.
3. S. Wagner, A. Keith and W. Snipes (1980), Biochim. Biophys. Acta 600, 367-375.

W-AM-C9 THE EFFECTS OF AXIAL MOTION AND ORIENTATION DISTRIBUTIONS ON EPR AND SATURATION TRANSFER EPR SPECTRA. Carl F. Polnaszek and David D. Thomas, Department of Biochemistry, University of Minnesota, Medical School, Minneapolis, MN 55455 (Intr. by D. Levitt).

Simulations of the saturation transfer EPR V_2' spectra of ^{14}N nitroxide spin probes have been extended to include the usual non-axial magnetic g and hyperfine interactions. The motional model is that of rotation about a single axis in the molecule (axial motion). This model had been previously applied to analyze the conventional EPR spectra in such systems as gel-phase membranes. The calculations were performed (a) for single orientations of the probe axis with respect to the magnetic field, which are appropriate for the analysis of STEPR spectra obtained in oriented systems and also (b) for a random distribution of probe orientations found in most experimental situations. Calculations were performed for z-axis motion, suggested for fatty acid spin probes and some proteins, and y-axis motion, appropriate for the cholestane spin probe. Comparison with published data suggests that there is significant off-axial motion with a rate greater than 10^3/sec occuring with fatty acid probes. The y-axis axial motion predictions appear to be appropriate to several experimental cases.

Calculations of the conventional EPR spectra of oriented systems in the rigid limit have been extended to include non-axial magnetic tensors. The results show that conclusions about the preferred orientation of the probe and the spread of the distribution around this angle can change quite markedly when simulations include the correct hyperfine and g values. Inclusion of an orientation distribution on the second or azimuthal angle suggests that measured g-values can be used to obtain parameters for this distribution.

W-AM-C10 MOTIONAL PROPERTIES OF SPIN LABELS IN PROTEINS: EFFECTS OF HYDRATION

J. Ruggiero*, R. Sanches, M. Tabak and O.R. Nascimento
*Instituto de Biociências, Letras e Ciências Exatas - UNESP - S.José do Rio Preto, SP
Instituto de Física e Química de São Carlos - USP - S.Carlos, SP - Brazil.

Conventional and saturation transfer ESR techniques are used to study the motional properties of several spin labels introduced in three proteins: lysozyme, sperm whale myoglobin and human hemoglobin. The mobilities of a maleimide spin label which binds covalently to the proteins, as well as of two small probes TEMPO and PD-TEMPOL were monitored in the temperature range -10^{o}C to -150^{o}C for samples in the dry and solution states. The three proteins show a similar temperature dependence as indicated by the parameters $2A_{zz}$ and ΔH. A small linear increase in $2A_{zz}$ with the decrease in temperature is observed for the dry samples. For the proteins in solution, on another hand, the $2A_{zz}$ temperature dependence shows a change of behavior around -60^{o}C which is related to the freezing of the water molecules in the hydration shell. The changes observed for the parameter ΔH are such that at temperature below -60^{o}C ΔH is greater for the solution sample while at temperatures above -60^{o}C ΔH is greater for the dry sample. ST-ESR measurements show that the motion of the spin label is very restricted in all systems ($\tau_c > 10^{-5}$ sec) in the temperature range studied, so that the residual librational motion of the label is sensitive to the hydration being responsible for the observed changes of the ESR parameters with temperature.

W-AM-D1 "METHODS FOR THE DETERMINATION OF MOLECULAR ACCESSIBLE SURFACE AREA CHANGES IN PROTEIN DENATURATIONS OR DRUG-BIOMOLECULE ASSOCIATIONS FROM DATA OF EXPERIMENTS IN A RANGE OF MIXED SOLVENTS", By: O. Sinanoğlu, Yale Univ., (Intr. by D.M. Crothers)

Secondary, tertiary, and higher structure formations of biopolymers as well as associations of drug, nucleotide base, and other biomolecules in solution are crucially affected by the strong "solvophobic forces", a combination of four clear-cut free energy effects which exist in water as well as in other solvent media though to a lesser extent in the latter. These forces were introduced, along with the concept and methodology of molecular surface areas exposed to solvent, earlier [O. Sinanoğlu, in "Molecular Associations in Biology", (1968) (B. Pullman, Editor); Academic Press, N.Y. pp. 427-455)]. The potentials of these "forces" involve the microscopic surface tension down to molecular dimensions of the solvent cavity "walls" (ΔG_c) surrounding protein side chains, etc., together with the "interaction free energies", ΔG_{int} of the solute pieces with the solvent molecules around. A theory for the interactions were also given but were more cumbersome to use than the new formulation that will be presented here, involving instead of the $\Delta G_c + \Delta G_{int}$, a "differential microsurface tension" which can be determined from HPLC experiments such as the ones of Horváth and Melander. Using the eluent-biomolecule values thus obtained, the accessible surface area changes $\Delta\sigma$ of processes like protein folding are evaluated readily from denaturation microcalorimetric data or from van't Hoff plots-data in a range of mixed solvents. The lysozyme data of Sturtevant and Veliçelebi in a wide range of methanol-water mixtures give for example the $\Delta\sigma$ of denaturation as (+ 169Å^2) per molecule, while the actinomycin-deoxyguanosine association data of Crothers and Ratner gives a $\Delta\sigma$ of (-36.4Å^2).

W-AM-D2 MOLECULAR DYNAMICS SIMULATION OF SUGAR PUCKERING IN PHENYLALANINE TRANSFER RNA. M. Prabhakaran and Stephen C. Harvey, Department of Biochemistry, University of Alabama in Birmingham, Birmingham, AL 35294.

Our 24 psec molecular dynamics simulation of yeast phenylalanine transfer RNA[1-4] provides an opportunity to examine structures and energetics of sugar pucker, and the spontaneous repuckering of two sugars (ribose 46 and ribose 76) gives information on the kinetics and pathways of repuckering. In contrast with earlier studies using static structures and energy minimization, the simulation gives a proper statistically distributed ensemble of structures for analysis. The expected pseudorotational pathway between the southern (S) hemisphere or C2'-endo-like conformation and the northern (N) or C3'-endo-like conformation is followed, via the S-E-N path rather than the S-W-N path, and with the pucker amplitude in the range of 30° to 60°. We have examined the correlations between the various torsional angles and sugar pucker, as well as between bond angles and pucker angle, and the structures have been used to compare the dependence of conformational energy on pucker for the parameter proposed by Levitt[5], Olson[6], and Kollman[7].

1. M. Prabhakaran et al., J. Biomolec. Struct. Dyns. 1, 357 (1983).
2. S.C. Harvey et al., Science 223, 1189 (1984).
3. S.C. Harvey et al., Biopolymers, in press.
4. M. Prabhakaran et al., Biopolymers, in press.
5. M. Levitt and A. Warshel, J. Amer. Chem. Soc. 100, 2607 (1978).
6. W.K. Olson, J. Amer. Chem. Soc. 104, 278 (1982).
7. S.J. Weiner et al., J. Amer. Chem. Soc. 106, 765 (1984).

W-AM-D3 MAGNETIC CIRCULAR DICHROISM OF CYTOSINE AND THYMINE TO 180 nm. John Clark Sutherland, Bohai Lin*, JoAnn Mugavero and John Trunk. Biology Department, Brookhaven National Laboratory, Upton, NY 11973[t]

We have extended measurements of the magnetic circular dichroism (MCD) of cytosine and thymine, both at neutral pH, to about 180 nm in the vacuum ultraviolet. Previous MCD measurements stopped at 220 and 210 nm respectively (Voelter et al., JACS 90, 6163; 1968). For thymine, we find a trough at 190 nm in addition to the previously reported peak at 215 and trough at 263 nm. This result indicates that the absorption band with a peak at 205 nm is composed of at least two non-parallel electronic transitions. For cytosine, we find a peak at about 195 nm and a trough at 210 nm in addition to the previously reported troughs at 235 and 270 nm. Thus the absorption peak just below 200 nm has a transition dipole that makes a large angle with the transition dipoles of the three longer wavelength transitions which are approximately parallel. The wavelengths, directions and intensities of the electronic transitions of the bases are critical for interpretation of the natural CD spectra of DNA and RNA.

* Permanent address: Institute of Biophysics, Academia Sinica, Beijing, China.

[t] Research sponsored by the U.S. Department of Energy. MCD experiments were performed at the National Synchrotron Light Source, also supported by the U.S.D.O.E.

W-AM-D4 DIFFUSION-ENHANCED ENERGY TRANSFER TO DNA-ASSOCIATED CHROMOPHORES. Theodore G. Wensel and Claude F. Meares, Department of Chemistry, University of California, Davis, California 95616.

Information about the equilibrium properties of intercalators bound to DNA, or colored ions electrostatically attracted to DNA, may be gained from studies of intermolecular energy transfer. These employ small, freely diffusing complexes of terbium whose electric charge can be made +1, 0, or -1 with minimal change in structure. During its millisecond lifetime, an excited terbium complex in aqueous solution can diffuse through $\sim 10^4$ Å and sample a large number of environments; effects on its lifetime due to the presence of energy acceptors in the solution thus provide equilibrium information about minimum distances of donor-acceptor separation and about electrostatic effects on radial distribution functions. Probes with (+1, 0, -1) charge have been used to study ethidium, acridine, and cobalt-bleomycins bound to DNA; and also to study small transition-metal complexes with (+1, 0, -1) charges in the presence of DNA. Results are being compared with theoretical predictions.

W-AM-D5 EFFECT OF DNA BASE COMPOSITION AND SEQUENCE ON THE BINDING AFFINITY OF DAUNOMYCIN. David P. Remeta, Mary M. Senior, Barbara L. Gaffney, Roger A. Jones, and Kenneth J. Breslauer, Department of Chemistry, Rutgers University, New Brunswick, NJ 08903

Daunomycin is a member of the class of glycosidic anthracycline antibiotics which are effectively used in combination chemotherapy for the treatment of acute leukemia and a wide variety of solid tumors in man. The cytotoxicity of daunomycin appears to result from its putative mode of binding to DNA and consequent inhibition of the cellular replication and transcription processes. To determine the relative affinity and base sequence specificity of the antibiotic-DNA interactions, our laboratory is currently investigating the binding of daunomycin to selected oligomeric and polymeric DNA duplexes. Employing spectroscopic and microcalorimetric techniques, we have thermodynamically characterized the binding of daunomycin to salmon testes DNA, and to the alternating copolymers poly d(AT)·poly d(AT) and poly d(GC)·poly d(GC). Preliminary results indicate that the drug does not exhibit a preferential affinity for either d(GC) or d(AT) base pairs in the polymeric host duplexes. In fact, the binding free energies, enthalpies, and entropies for daunomycin-DNA complex formation reflect no significant sequence dependence. However, these thermodynamic binding profiles include contributions from both local drug-DNA interactions and any long-range drug-induced conformational changes. To resolve these two contributions thermodynamically, we are studying the interaction between daunomycin and the self-complementary deoxyoligonucleotides d(CGTACG) and d(CGCGCG) which contain single binding sites and therefore preclude long-range effects. The results of these investigations will be reported and discussed in terms of the influence of base composition, sequence, and local versus long-range effects on the thermodynamic profiles of the binding process.

W-AM-D6 LONG-RANGE ALLOSTERIC EFFECTS ON THE B TO Z TRANSITION BY DAUNOMYCIN. J. B. Chaires, Department of Biochemistry, The University of Mississippi Medical Center, Jackson, MS 39216-4505

Previous results from this laboratory have established that the anthracycline antibiotic daunomycin will inhibit the salt-induced transition of poly d(G-C) from the B form to the left-handed Z form. Binding of daunomycin to poly d(G-C) under solution conditions that favor the Z form is cooperative, a finding that is consistent with a model in which the drug preferentially binds to the B form, and acts as an allosteric effector on the B to Z equilibrium. Recent studies have used circular dichroism, sedimentation, and enzymatic methods to directly demonstrate the structural alteration in the DNA previously inferred from binding studies. The amounts of bound drug required to convert Z DNA back to the B form was found to be strongly dependent on the ionic strength. Under certain solution conditions, that would otherwise favor the Z form, as little as one molecule of daunomycin per 25 base paires is sufficient to convert poly d(G-C) entirely to the B form. This is a striking example of a long-range allosteric effect on DNA conformation, of interest in its own right, as well as in terms of understanding the mechanism by which daunomycin acts to inhibit transcription and DNA replication. Supported by National Cancer Institute Grant Ca 35635-01A1.

W-AM-D7 NETROPSIN BINDING TO DNA OLIGOMERS WITH ONE BINDING SITE.
Luis A. Marky and Kenneth J. Breslauer, Department of Chemistry, Rutgers-The State University, New Brunswick, New Jersey, 08903.

Thermodynamic binding profiles for complexation of a drug with a DNA polymer duplex may contain contributions from both local drug-DNA interactions and long-range drug-induced changes in the host duplex. We have thermodynamically characterized the binding of netropsin (a B-conformation minor groove ligand) to a series of polymer host duplexes [Biophysical Journal 45, 235a, (1984)].

To separate the contributions of local netropsin - DNA interactions from longer range drug-induced changes, we have optically and calorimetrically investigated the binding of netropsin to a series of oligomeric duplexes containing a single binding site. Specifically we have studied the binding of netropsin to the duplexes formed by the sequences: d(GGAATTCC), d(GGTATACC), d(GGCATGCC).

We note the following trends. a) netropsin binding increases the thermal stability of the host duplexes in the following order: d(GGAATTCC) ∿ d(GGTATACC) > d(GGCATGCC). Binding free energies are calculated from the Δt_m data. b) For all the oligomers noted we observe exothermic binding enthalpies. Specifically, the exothermicity of netropsin binding decreased in the order: d(GGAATTCC) > d(GGTATACC) > d(GGCATGCC). These thermal data will be discussed in the terms of molecular models of netropsin-DNA interactions derived from x-ray and NMR studies. This work was supported by NIH GM-23509.

W-AM-D8 INHIBITION OF RESTRICTION ENZYME DIGESTION OF PBR322 FRAGMENTS BY THE CARCINOGENS 4-NITROQUINOLINE-1-OXIDE AND N-ACETOXY-N-ACETYL-2-AMINOFLUORENE. **Stephen A. Winkle, Nicholas Combates, Brian Latario, Gary Langieri, Michael Mallamaci and Megerditch Kiledjian Department of Chemistry Rutgers University New Brunswick, NJ 08903.**

Previous studies suggest that the carcinogens 4-Nitroquinoline-1-Oxide (NQO) and N-Acetoxy-N-Acetyl-2-Aminofluorene (AAAF) bind preferentially to certain regions on the DNAs pBR322 and ΦX174RF (S.A. Winkle, M. Mallamaci, D.P.Reed [1983] Biophys. J. 41, 287a; S.A. Winkle, et. al. [1984] Biophys. J. 45, 289a). To further locate these high affinity NQO and AAAF binding sites on pBR322, we have investigated the inhibition of digestion of fragments containing these sites by certain restriction enzymes when NQO or AAAF is bound to the fragments. PBR322 was reacted with increasing concentrations of either NQO or AAAF, the DNA was digested with a restriction enzyme and the fragments isolated by gel electrophoresis. (Fragments containing no bound carcinogen were also isolated.) Fragments were then reacted with a second restriction enzyme. The electrophoresis gels of the products of these second enzyme digestions suggest that, with fragments containing previously suggested high affinity binding sites, certain restriction enzymes are inhibited. For example, the Hinf I-154 base pair (bp) fragment appears to contain hot spots for both NQO and AAAF. With both carcinogens, the cutting of this fragment by the restriction enzyme Hha I into subfragments of 97 and 57 bp is inhibited. Inhibition increases as the concentration of bound carcinogen increases. In all cases, inhibition of restriction enzyme activity (e.g. Hha I, Alu I) has been observed for hot spot-containing fragments in areas of high GC content with continuous GC sequences. This work supported by NCI grant CA 34762.

W-AM-D9 THE EFFECT OF SOLVENT VISCOSITY AND TEMPERATURE ON DNA VISCOELASTIC BEHAVIOR.
J.Y. Ostashevsky and C.S. Lange, SUNY Downstate Medical Center, Brooklyn, NY 11203.

The effect of solvent viscosity (η_s) and temperature (T) on the shape of the concentration dependence of the principal and total recoils in creep-recovery viscoelastometry experiments has been studied for T4 DNA solutions. The range of DNA concentration (c) was 2 - 50 μg/ml; glycerol, 70 - 80 %v/v, sucrose, 60 %v/v; NaCl, 5 mM - 1 M; and T, 275 - 323°K. A linear proportionality between recoil and c was obtained at high η_s/T. At low η_s/T, the c-dependence was nonlinear, approaching saturation at higher c. At low c, the slope of both curves was the same. Transition between linear and nonlinear values occurred over a narrow range of η_s/T (a width of 1 - 5°K if η_s/T was changed by varying T). $(\eta_s/T)_{crit}$, the midpoint of the transition, was independent of solvent properties other than viscosity. Also, $(\eta_s/T)_{crit}$ increased with c and decreased with ionic strength (μ). The retardation time, τ, was proportional to η_s/T as predicted by Zimm's theory (1). The observed transitions can be explained qualitatively by De Gennes's theory for concentrated polymer solutions (2), comparing τ and T_R, the lifetime of the contact points of the polymer network. The nonlinear values are consistent with a pseudogel which exists when $\tau < T_R$ (3). At $\tau > T_R$, the DNA behavior is similar to that in dilute solutions (linear values). Thus, the condition for transition is $\tau = T_R$. Theory predicts that T_R increases with c and molecular size (varied in our experiments by decreasing μ). This agrees with our data. Also, T_R can change cooperatively (4), which would explain the narrow width of the transition. However, it remains unclear how T_R can change with η_s/T in a different way than does τ ($\tau \sim \eta_s/T$). This work supported by a grant from The Mathers Charitable Foundation.
(1) L.C. Klotz & B.H. Zimm (1972) Macromolecules 5:471; (2) P.G. De Gennes (1976) ibid. 9:594; (3) M. Adam & M. Desanti (1977) ibid. 10:1229; J. Klein (1978) ibid. 11:852.

W-AM-D10 GEL ELECTROPHORES OF DNA USING PULSED ELECTRIC FIELDS Nauzer Kalyaniwalla and Charles P. Bean, Physics Dept., Rensselaer Polytechnic Institute, Troy, NY 12180

Following the lead of Jamil and Lerman[1], we have measured the average motion of Hind III split fragments of λ phage DNA in pulsed electric fields. It is well known that, in steady state, the mobility of large fragments of DNA increases significantly for fields as low as 1 V/cm[2,3]. We have used fragments of up to 23,100 base pairs in fields to 15 V/cm with pulse lengths on the order of a second. For brief pulses the mobility approaches the low field limit. The relaxation time for the mobility to approach the steady state limit increases with the length of the fragment and decreases with increasing field. The effect can be used to maximize the resolution of gel electrophoresis in a given region of molecular weight of DNA. It represents a special case of the technique of Schwartz and Cantor[4] in which a uniform applied field is employed as contrasted to their non-uniform fields.

1. Tahir Jamil and Leonard S. Lerman, State University of New York at Albany (unpublished).
2. M.W. McDonell, M.N. Simon and F.W. Studier. J. Mol. Biol. 110, 119 (1977).
3. O.J. Lumpkin and B.H. Zimm. Biopolymers 21, 2315 (1982).
4. D.C. Schwartz and C.R. Cantor. Cell 37, 67 (1984).

W-AM-D11 DYNAMICS OF COUNTERION POLARIZATION IN THE VICINITY OF A SHORT DNA RESTRICTION FRAGMENT AS CHARACTERIZED BY FIELD REVERSAL ELECTRIC BIREFRINGENCE. DON EDEN, MATHEEN HALEEM, AND AKEMI KOUYAMA. DEPT. OF CHEMISTRY, SAN FRANCISCO STATE UNIVERSITY, SAN FRANCISCO, CA 94132.

Field reversal transient electric birefringence experiments have been performed on a 104 basepair restriction fragment obtained from sites 298-402 of pBR322 using an improved apparatus with 10 ns resolution. The transient that occurs upon field reversal has been analyzed using the theoretical approaches of Tinoco and Yamaoka (J. Phys. Chem. 63, 423 (1959)) and Takezoe and Yu (Biochemistry 20, 5275 (1981)) in order to obtain the relaxation time, τ_μ, associated with the induction of a slow induced dipole moment that arises from the displacement of counterions in an applied field. Measurements in a phosphate buffer 1 mM in Na^+ over a temperature range of 3 to 25 C yield τ_μ's that scale with solution viscosity, indicating that the process is diffusively driven. Experiments in a neutral buffer in the presence of 0.5 mM Mg^{++} have relaxation times almost the same as that of Na^+. Since the electrical mobility of Mg^{++} is only 6% greater than that of Na^+ and since Mg^{++} is expected to associate much more strongly than Na^+ with the DNA, the similarities in the τ_μ's suggests that the dipole moment is induced principally by the displacement of ions relatively far from the helix. Using Takozoe and Yu's theory we determine that τ_μ is approximately 150 ns at 3 C. This is in excellent agreement with the predictions of Mandel (Mol. Phys. 4, 489 (1961)), if the bulk solution values for the translational diffusion constant of the counterions is used.

This research was supported by NIH grant GM 31674 and a Research Career Development Award to DE.

W-AM-D12 LIQUID CRYSTALLINE AND CRYSTALLINE PHASES OF SODIUM DNA IN AQUEOUS SOLUTION. Randolph L. Rill, Dept. of Chemistry and Institute of Molecular Biophysics, The Florida State University, Tallahassee, FL 32306.

Concentrated aqueous saline solutions of relatively short, defined length (147 nucleotide pairs) DNA fragments at room temperature suddenly become turbid and iridescent when the DNA concentration is increased or temperature is decreased beyond critical values. Microscopic examination through crossed polarizers shows that turbidity and iridescence is caused by DNA spherulites suspended in an isotropic phase. This behavior indicates formation of a liquid crystalline DNA phase similar to cholesteric liquid crystals formed in non-aqueous solutions by semi-rigid, non-electrolyte polymers such as polybenzyl-L-glutamate. Upon cooling the liquid crystalline phase coalesces to form DNA crystals. Relatively large crystals are formed by slow cooling under near equilibrium conditions. A partial phase diagram has been obtained for the isotropic --> liquid crystal --> crystal transitions of 147 np DNA in buffered saline (0.1 M Na^+) by measuring changes in visible light transmission of solutions in the presence and absence of crossed polarizers as functions of temperature and DNA concentration. Biphasic, anisotropic + liquid crystalline solutions are observed at concentrations above ca. 170 mg/ml and temperatures above ca. 23°. DNA crystals, in equilibrium with anisotropic solution, are formed at concentrations as low as 100 mg/ml and temperatures below ca. 23°.

This work was supported in part by grants from NIH (GM 29778) and the Department of Energy (EV05888).

W-AM-E1 COMPARISON OF SECONDARY STRUCTURES OF PROTEINS IN THE SOLID STATE AND IN SOLUTION BY RESOLUTION-ENHANCED FT-INFRARED SPECTROSCOPY. D. Michael Byler and Heino Susi (Intr. by George C. Na), Eastern Regional Research Center, U. S. Department of Agriculture, Philadelphia, PA 19118.

The unresolved amide I band in the infrared spectra of proteins consists of a number of component bands. Resolution enhancement of the spectrum by Fourier self-decovolution and second derivative techniques provides detailed information on the frequencies and intensities of the individual components. The amide I vibrations of the peptide groups of protein segments with different secondary structures (e.g., α-helix and β-strand) exhibit different characteristic absorption frequencies. The band areas of the individual components, as measured by Gauss-Newton iterative curve-fitting methods, are proportional to the relative amounts of the various types of conformation found in the protein.

Comparison of the spectra for a given protein taken in solution as well as in the solid state demonstrates that there are clearly observable differences between the conformations of the protein in these two states. Usually fewer components are observed in the spectra for the solid state than solution. In addition, the constituent features are frequently broader and often display shifts in frequency and changes in band area. Such variations can be associated with differences in the hydrogen-bonding interactions and type of folding in the two states of the protein. The structure and spectra of the proteins chymotrypsin and myoglobin, among others, will be discussed in some detail.

W-AM-E2 ^{13}C-NMR STUDIES OF THE STRUCTURE AND DYNAMICS OF M13 COAT PROTEIN. Gillian D. Henry, Joel H. Weiner and Brian D. Sykes, Department of Biochemistry, University of Alberta, Edmonton, T6G 2H7 CANADA.

The filamentous coliphage M13 possesses multiple copies of a 50-residue coat protein which is deposited as an integral membrane protein in the inner membrane of *E. coli* during infection. The coat protein possesses the sequence of a typical membrane protein, comprising a 20-residue highly hydrophobic core flanked by hydrophilic regions. We have examined the structure and backbone motions of M13 coat protein in two detergent systems, SDS and deoxycholate.

M13 coat protein contains 10 alanine residues distributed throughout all 3 domains. Biosynthetic incorporation of 3-(^{13}C)alanine has provided an overall view of the protein. Resonance assignments were made by pH titration (ala-1) and limited proteolysis. Relaxation data (T_1, T_2, NOE) have been analysed according to the model-free approach of Lipari and Szabo (JACS 104: 4546) yielding a dynamic picture of the molecule. This label suggests the structure to be similar in both detergents; the hydrophobic core residues approach rigidity (the order parameter, S^2, approaches 1) and the hydrophilic domains are also well-structured. Least order is apparent at the extreme ends (ala-1 and ala-49).

A variety of carbonyl labels (lysine, tyrosine, phenylalanine and proline) have been similarly incorporated. The various contributions to relaxation have been assessed; in contrast to protonated carbons, the dipolar term no longer predominates. The sensitivity of the carbonyl carbon chemical shift to the protonation or deuteration state of the amide nitrogen has provided information on relative exchange rates at several amide nitrogens.

W-AM-E3 QUENCHING OF THE INTRINSIC FLUORESCENCE OF LIVER ALCOHOL DEHYDROGENASE BY COENZYME BINDING AND BY THE ALKALINE TRANSITION. Maurice R. Eftink, Department of Chemistry, The University of Mississippi, University, MS 38677.

The fluorescence of horse liver alcohol dehydrogenase (LADH) is quenched by the acid dissociation of some group on the protein having an apparent pK_a = 9.6 at 25°C. The pK_a of this alkaline quenching transition is unchanged by the binding of trifluoroethanol or pyrazole to the enzyme or by the selective removal of the active site Zn^{+2} ion. This indicates that the ionization of a zinc bound water molecule is not responsible for the quenching. The binding of NAD^+ to the enzyme causes a drop in protein fluorescence and an apparent shift in the alkaline quenching transition to lower pH. In the ternary complex formed with NAD^+ and trifluoroethanol the alkaline transition is difficult to discern between pH 6-11. In the NAD^+-pyrazole ternary complex, however, a small but noticeable fluorescence transition is observed with a pK_a (app) $\approx$ 9.5. We propose that the alkaline transition centered at pH 9.6 is not shifted to lower pH upon binding NAD^+. Instead the amplitude of the alkaline quench is decreased to the point that it is difficult to detect when NAD^+ is bound. We present a model which describes the dependence of the fluorescence of the protein on pH and NAD^+ concentration in terms of two independently operating, dynamic quenching mechanisms. Our data and model cast serious doubt on the identification, made previously in the literature, between the alkaline quenching pK_a and the pK_a of the group whose ionization is coupled to NAD^+ binding. Also, simulations demonstrate that the apparent pK_a values, obtained for LADH from plots of fluorescence intensity versus pH, are underestimates of the true pK_a values. The true pK_a for the alkaline quenching transition is found to be 9.9 at 25°C. Supported by NSF grant PCM-82-06073.

W-AM-E4 STUDIES OF THE TEMPERATURE AND VISCOSITY DEPENDENCE OF THE SOLUTE QUENCHING OF THE TRYPTOPHANYL FLUORESCENCE OF COD PARVALBUMIN. Maurice R. Eftink and Karen A. Hagaman, Department of Chemistry, The University of Mississippi, University, MS 38677.

The use of solute quenchers, such as acrylamide and molecular oxygen, to quench the fluorescene of internal tryptophanyl (trp) residues in globular proteins has provided valuable insights regarding the dynamics of protein structures. Cod Parvalbumin is a protein that possesses a single trp residue, which from its fluorescence characteristics ($\lambda_{em} \approx 315$nm), is apparently buried from solvent. We have studied the solute quenching of the trp fluorescence of parvalbumin and have found dynamic quenching rate constants, k_q, (i.e. from lifetime Stern-Volmer plots; τ_o = 3.3 nsec) of 1.1 x $10^8 M^{-1}s^{-1}$ and 2.3 x $10^9 M^{-1}s^{-1}$ with acrylamide and oxygen, respectively, at 25°C. These rate constants are among the lowest values that have been found for the quenching of trp fluorescence in proteins by the respective quenchers. From temperature dependence studies, activation enthalpies of 6.5 $\pm$ 1.5 and 6.0 $\pm$ 0.5 kcal/mole are found for acrylamide and oxygen quenching. The k_q for acrylamide quenching is found to be relatively unchanged ($\pm$ 10%) by a 5-fold increase in the bulk viscosity (glycerol-water mixture). These temperature and viscosity studies argue that the acrylamide quenching process involves a dynamic penetration of the quencher, facilitated by fluctuations in the protein's structure. While there is little change in the acrylamide k_q on increasing the bulk viscosity from 1 to 10 cP, a further increase from 10 to 100 cP results in a significant reduction (3-fold drop) in k_q. This indicates that at high viscosity that either a) the fluctuations in the protein structrue are dampened by the surrounding viscous solvent, and/or b) that the rate limiting step becomes diffusion of the quencher through the solvent and not through the protein matrix. Supported by NSF grant PCM-82-06073.

W-AM-E5 NMR STUDIES OF E.COLI THIOREDOXIN UTILIZING SELECTIVE 13C, 15N, AND 2H ENRICHMENT. David M.LeMaster* and Frederic M.Richards, Dept. of Molecular Biophysics and Biochemistry, Yale University, New Haven, CT 06511

We have produced a series of E.coli thioredoxin samples (M.W.=11,675) enriched by residue type via growth of auxotrophic bacteria on amino acids possessing various labeling patterns. The majority of amide protons have been observed as individual resonances utilizing the J1 spin coupling to 15N in selectively enriched samples. Assignment of interresidue connectivities have proven feasible by observing the selective NOE of enriched main chain carbonyl resonances due to the amide protons of the following residue. This approach offers certain advantages over the standard NOE experiment which utilizes interactions between the amide proton and the alpha and beta protons of the preceding residue. Solvent suppression is unnecessary. The interaction is between nuclei separated by a constant distance rather than those whose distance is dependent on conformation. These factors routinely give rise to ambiguities and errors in connectivity assignments in the standard approach. In our effort to establish intraresidue spin connectivities in the carbon spectra, we have also produced thioredoxin samples containing residues uniformily 13C enriched to 99% suitable for 13C-13C 2D J-resolved and chemical shift correlation experiments.
(Supported by grants NIH GM-22778 and NSF PCM-8305203.)

W-AM-E6 DISTANCE MEASUREMENTS IN SPIN-LABELED LYSOZYME AND BOVINE PANCREATIC TRYPSIN INHIBITOR. Paul G. Schmidt and Irwin D. Kuntz; Vestar Research Inc., Pasadena, CA 91106 (PGS) and University of California, San Francisco, San Francisco, CA 94143 (IDK).

The time-averaged structure of any molecule can be determined if one measures a sufficient number of interatomic distances. Distance geometry (Kuntz, et. al. (1979) Biopolymers 18, 939-957) provides the mathematical framework to convert distance measurements, with the associated experimental errors, into actual three-dimensional structures. Two-dimensional NMR techniques (NOESY) can provide a large number in interproton distances in small proteins. But these distances are all relatively short, leaving the structure underdetermined. Larger distances can be gauged from the relaxation enhancement afforded by paramagnetic loci. We have begun a systematic test of covalently bound spin labels for distance measurements in small proteins using hen egg white lysozyme and BPTI. ^{1}H NMR spectra of lysozyme spin-labeled at His-15 contain peaks specifically broadened by the nitroxide free radical. Difference spectra after ascorbate reduction reveal nearby groups. The difference spectrum amplitudes are related in a simple way to r^{-6} where r is the label-to-proton distance. Using distance geometry to solve for the nitroxide location yielded a well defined position for the label in a hydrophobic groove between Phe-3 and Asp-87. BPTI was labeled at amino groups and separated by HPLC into specific mono-labeled derivatives. One of these was examined at 500 MHz by the 2-D NMR COSY technique. Difference COSY after ascorbate reduction of the label yielded semiquantitative protein-label distances. Distance geometry placed the label near Lys-26. While presenting a potential problem, motion of the label does not appear to degrade significantly the distance measurements.

W-AM-E7 REINVESTIGATION OF THE DIELECTRIC PROPERTIES OF HUMAN HEMOGLOBIN DURING OXYGENATION
Shiro Takashima, Department of Bioengineering, D3, University of Pennsylvania, Philadelphia, PA 19104

Some years ago, Takashima and Lumry observed that the dielectric constant of horse hemoglobin solution changed considerably with partial oxygenation. It increased to a maximum value at oxygen partial pressures which correspond to 25% and 75% saturation with a minimum between these two peaks. However, because of the difficulty of reproducing these data, the result has not been accepted generally. Recent studies by Battistel et al. indicate that the molar heat capacity of human hemoglobin showed a maximum value at 25% saturation and a broad hump near 75% oxygenation. This observation renewed the interest in the dielectric properties of partially oxygenated hemoglobin. We expanded the frequency range using a wide band amplifier and measurements were done between 10 KHz and 5 MHz. We found that partially oxygenated hemoglobin exhibited two relaxation processes while fully oxygenated hemoglobin showed only one. The new relaxation process which appears with partial oxygenation is variable depending upon oxygen partial pressure while the second relaxation which arises from the permanent dipole of Hb molecule remains constant during oxygenation. In spite of this new feature, the present work seems to confirm the original finding.

W-AM-E8 **COOPERATIVE DIMERIC AND TETRAMERIC CLAM HEMOGLOBINS HAVE MYOGLOBIN FOLDED SUBUNITS BUT ARE ASSEMBLED DIFFERENTLY FROM MAMMALIAN HEMOGLOBINS.**
William E. Royer, Jr. and Warner E. Love. Thomas C. Jenkins Department of Biophysics, Johns Hopkins University, Baltimore, MD 21218

The structure of crystals of the carbon monoxide complex of dimeric and tetrameric hemoglobins from the blood clam, Scafarca inaequivalvis have been determined at 5.5 A resolution. The subunits have an extra helix at the amino end of the chain, but otherwise are folded as sperm whale myoglobin. The tetramer is a dimer of dimers. The dimers are made by placing the E helix-heme-F helix faces of subunits in apposition. The contacting surfaces are such as to suggest a simple mechanism for the cooperativity observed in these hemoglobins.

We thank Dr. Emilia Chiancone for gifts of hemoglobin. This work was supported by NIH grant AM 02528.

W-AM-E9 USING TRANSFER ENERGIES TO PREDICT SOLVENT EXPOSURE AND CONFORMATIONAL HOMOLOGIES OF GLOBIN α HELICES.
H.Robert Guy, Lab of Mathematical Biology, N.C.I., National Institutes of Health, Bethesda, Md 20205.

The crystal structures for one or more members of five globin families all contain 7 or 8 α helices that are stacked in approximately the same manner. Comparison of vertebrate hemoglobin and myoglobin sequences to insect midge larva globin and plant leghemoglobin sequences reveals that few residues in structurally homologous positions are identical. Globin sequences were analyzed with a method that calculates optimal solvent exposure of α helix residues (H.R.Guy, 1984, Biophys. J., 45: 249). Analysis of known structures indicates that the calculation is very accurate for α helix residues that are more than three residues from an end of an α helix. Several quantities were calculated with this method; eg., location on α helical segments of water-protein interfaces, fraction of a helical segment that is buried, energies to transfer a helical segment from water and from the protein interior to its optimal postion, energy to completely bury a residue or segment, and energy to bury every other residue. The energy to transfer a seven-residue-long helical segment from water to its optimal position is more conserved among all globin sequences than other quantities calculated. This parameter may be useful for homology searches and in evaluating structural relationships among sequences that have few identical residues in homologous positions. It may be useful for investigating evolutionary trees; eg., these calculations suggest that leghemoglobins are more closely related to frog muscle α hemoglobin and bloodworm globin than to midge larva globins. This prediction is consistent with patterns of exons and introns in different globin DNA sequences.

W-AM-E10 HEPARIN MODULATES CONFORMATIONAL STATES OF PLASMA FIBRONECTIN: A SPIN LABEL APPROACH

E. G. Ankel[1], C.-S. Lai[1], G. Homandberg[2] and N. M. Tooney[2]

[1]National Biomedical ESR Center, Department of Radiology, Medical College of Wisconsin, 8701 Watertown Plank Road, Milwaukee, Wisconsin 53226, and [2]Department of Medicine, University of Wisconsin Medical School, Milwaukee Clinical Campus, Milwaukee, Wisconsin 53201.

Plasma fibronectin, a 440,000-dalton glycoprotein, normally present in plasma has specific binding sites for a number of biologically important materials, including heparin, collagen and cell surface. We have examined the interaction between heparin and human plasma fibronectin using electron spin resonance (ESR) spin label methods. The titratable sulfhydryl groups of plasma fibronectin were modified with a maleimide spin label [Lai and Tooney (1984) Arch. Biochem. Biophys. 228, 465-473]. Addition of heparin resulted in a decrease in the maximum splitting value of the ESR spectrum of spin-labeled fibronectin from 66.8 G to 64.3 G, suggesting that heparin induces a conformational alteration of plasma fibronectin. Other sulfated carbohydrates tested: dextran sulfate was found to be as effective as heparin but chondriotin sulfates were ineffective. The results presented suggested that the binding of heparin changes the molecular conformation of plasma fibronectin to a more relaxed or flexible state.

[Supported in part by an NIH grant No. 28444.]

W-AM-E11 AGGREGATION OF TUBULIN INDUCED BY TRIFLUOROETHANOL. J.J. Correia and R.C. Williams, Jr. Dept. of Molecular Biology, Vanderbilt University, Nashville, Tenn. 37235

Bayley et al. [Biopolymers 22, 87 (1983)] have recently demonstrated the ability of tubulin to attain conformations with high helical content in mixed apolar solvents, including 2[N-morpholino]-ethane sulphonic acid (MES) buffers with increasing concentrations of trifluoroethanol (TFE). We have confirmed these results under various buffer conditions and have demonstrated that increasing concentrations of TFE (0-80%) induce an increase in the α-helicity of tubulin (~24-66%) and also induce an increase in the extent of aggregation of the protein which causes the apparent molecular weight of the protein in solution (as measured by gel filtration studies with Sephacryl S-400) to increase from 1.0×10^5 to 1.3×10^6 Daltons. The molecular weight distributions observed are relatively paucidisperse and surprisingly insensitive to the initial protein concentration. Both the conformational transitions and the association phenomena are not reversed when TFE is removed. SDS PAGE performed in the absence of reducing agent indicates that this irreversibility is not due to disulfide linkages. These aggregates are not similar to tubulin aggregates formed during non-denaturing PAGE [Correia, J.J. and Williams, R.C., Jr., Biophysical J. 45, 374a (1984)]. Furthermore, these transitions are not involved in microtubule formation, but may be important for the association of tubulin with membranes. Previous studies indicate similar conformational transitions in tubulin structure when it is incorporated into phospholipid vesicles [Kumar et al., J.B.C. 256, 5886 (1981)]. Assembly may be mediated by the interaction of α-helices or coiled coils as is the case with keratins and intermediate filaments. (Supported by NIH Grant GM 25638.)

W-AM-E12 FLUORESCENCE ENERGY TRANSFER DISTANCES BETWEEN ACTIVE SITES IN *E. COLI* GLUTAMINE SYNTHETASE AND IN STACKED DODECAMERS Ann Ginsburg, Philip G. Kasprzyk, and Michael R. Maurizi, NHLBI, NIH, Bethesda, MD 20205

Glutamine synthetase (GS) from *E. coli* contains 12 identical subunits arranged in 2 superimposed hexagonal rings of ~ 140 Å in diameter with centers of subunits ~ 45 Å apart. ATP analogs that are modified at the 6 or 8 position of the adenine ring substitute for ATP in the autoinactivation reaction of Mn·GS at pH 7 with L-met-S-sulfoximine (M.R. Maurizi & A. Ginsburg, J. Biol. Chem. 257, 4271, 1982) and thereby can be fixed at enzyme active sites. Two fluorescent ATP donors, 8-mercapto ATP alkylated with N-(iodoacetylaminoethyl)-5-naphthylamine-1-sulfonic acid and 1-N^6-etheno-2-aza ATP, and two acceptors obtained by alkylation of 6- and 8-mercapto ATP with 4-dimethylaminophenyl-azo-phenyl-4-iodoacetamide (Y) were used. For fluorescence energy transfer measurements at pH 7.0, enzyme samples contained 1 or 2 eq of the same fluorescent donor per dodecamer and 6-Y-ADP, 8-Y-ADP, or ADP at remaining active sites. The distances calculated using the 4 combinations of donors and acceptors agreed well and indicated that active sites on GS are 49 or 57 Å apart if energy transfer occurs to 1 acceptor or to 2 equidistant acceptors, respectively. The latter value is close to the maximum distance of 60 Å possible between centers of active sites located on the outer edges of subunits heterologously bonded within a hexagonal ring. The location of active sites on exposed surfaces (which places active sites on isologously bonded subunits ~ 75 Å apart) was confirmed by using Zn^{2+} + 10 mM $MgCl_2$ at pH 7.0 to induce stacking of the same GS derivatives. The ensuing fluorescence quench indicated that intermolecular distances between active sites in stacked dodecamers is ~ 40 Å.

W-AM-F1 TRYPTIC MODIFICATION OF ERYTHROCYTE MEMBRANE Na,K-ATPase. William Harvey and Rhoda Blostein, Depts. of Biochemistry and Medicine, McGill University, Montreal, Canada.

The effect of trypsin treatment on human red cell Na,K-ATPase has been studied using inside-out membrane vesicles (IOV). Trypsin treatment in the presence of choline chloride cleaves the catalytic subunit (visualized by autoradiography of the phosphorylated intermediate following polyacrylamide gel electrophoresis in cationic detergent at acid pH) into 78 and 43 kilodalton fragments; sodium pump activity is decreased in a biphasic manner as a function of trypsinization time. These results are consistent with those observed by others using the purified kidney enzyme and with the conclusion that trypsinization of Na,K-ATPase in the E_1 form is associated with the loss of those activities believed to be associated with the $E_1P \rightleftarrows E_2P$ conformational transition step of the Na,K-ATPase. With IOV, concurrent measurement of initial rates of ATP-dependent $^{22}Na^+$ influx (normal efflux) and $^{86}Rb^+$ efflux (normal influx) indicate that trypsinization does not alter the Na/Rb stoichiometry. In addition concurrent measurements of pump modes reflected by the measurement of ATP-dependent $^{22}Na^+$ influx (normal efflux) show similar inactivation rates for Na/K exchange, anion-coupled Na^+ efflux and Na/Na exchange. Concurrent measurements of pump mediated Na/K exchange and Na,K-ATPase and of anion-coupled Na^+ efflux and Na-ATPase show an apparent uncoupling of ion transport from hydrolytic activity after trypsinolysis which is not readily explained on the basis of the relatively small increase in passive Na^+ and Rb^+ permeabilities caused by trypsin. (Supported by the MRC of Canada).

W-AM-F2 CARBODIIMIDES INHIBIT NA,K-ATPase BY FORMING INTRAMOLECULAR CROSS-LINKS. C. H. Pedemonte and J. H. Kaplan, Department of Physiology, University of Pennsylvania, Philadelphia, PA 19104

Treatment of dog kidney Na,K-ATPase enzyme with 1-ethyl-3(3-dimethylaminopropyl)carbodiimide (EPC) results in parallel, irreversible inhibition of Na-K-ATPase and PNPPase. Inhibition is first order with respect to time for all [EPC] tested. The I_{50} for ATP and PNPPase activities at 37°C was 1.7 mM and 2.5 mM respectively. The inhibition was unaffected by the presence of ATP, but greatly reduced by Mg, Na, K, choline or tris, in order of decreasing effectiveness. The inactivation kinetics indicate that the interaction of one molecule of EPC is sufficient for inhibition. Reaction with [^{14}C] glycine ethyl ester (GEE) subsequent to the addition of EPC indicated that carboxyl groups were modified by EPC as [^{14}C] incorporation occurred. Addition of GEE at the same time as EPC prevented inhibition of the enzyme, although [^{14}C] incorporation still took place. If GEE addition is delayed the initial inactivation is not reversed but little subsequent inactivation occurs. The protection against inactivation produced by GEE is not specific, other exogenous nucleophiles e.g. aminoethane and ethylenediamine are also effective. Although DCCD is a more potent inhibitor than EPC, similar protection by added nucleophiles was observed. It appears that after treatment with a diimide and nucleophile the Na,K-ATPase has modified carboxyl residues but is not inhibited, suggesting that the inhibition by diimide is due to reaction between the modified carboxyl and an endogenous nucleophile (a side-chain amine) and not by modification of the carboxyl per se. Formation of an intramolecular cross-link probably causes the inhibition with diimide resulting in an enzyme frozen in a non-functioning conformation. Supported by NIH HL 30315, AHA and NIH RCDA KO4-HL01092-03.

W-AM-F3 IDENTIFICATION, REVERSIBILITY, AND SENSITIVITY OF A Ca-DEPENDENT INHIBITIOR OF THE Na,K-ATPase OF HUMAN RED BLOOD CELLS. D.R. Yingst, D.M. Polasek and P.M. Polasek, Dept. of Physiology, Wayne State University, Detroit, MI 48201

The sensitivity of the Na,K-ATPase of human red blood cells to inhibition by Ca was increased 30 fold in the presence of a partially purified extract of human red cell hemolysate. The addition of the hemolysate fraction to the assay reduced the concentration of free Ca required for 50% inhibition from approximately 30 micromolar to less than 1 micromolar. The increased inhibition caused by the addition of the hemolysate fraction and the inhibition caused by Ca alone were reversible. Due to the presence of contaminating calmodulin, the hemolysate fraction also stimulated the Ca-ATPase and increased its affinity for Ca. In the presence of the hemolysate fraction the concentration of free Ca that inhibited the Na,K-ATPase by 50% was similar to that which half maximally stimulated the Ca-ATPase. Boiling the fraction destroyed its effect on the Na,K-ATPase, but did not impair its stimulation of the Ca-ATPase, substantiating previous results that calmodulin is stable and the inhibitor is labile at elevated temperatures. A protein which may be responsible for increased Ca-dependent inhibition of the Na,K-ATPase has been identified on SDS PAGE as a 30,000 dalton peptide. This protein binds to DEAE Sephadex at low ionic strength and can be selectively eluted by increasing the free Ca from less than 0.1 micromolar to 2 micromolar at a constant but elevated salt concentration. Since this protein could regulate the sensitivity of the Na,K-ATPase to inhibition by Ca, we have named it "calnaktin." [Supported by NIH (GM 3223-01A1), a SRF from AHA of MI to P.M.P., and a RCDA from NIH (AM 01253-01) to D.R.Y.]

W-AM-F4 HIGH-AFFINITY AND LOW-AFFINITY VANADATE BINDING TO SARCOPLASMIC RETICULUM CaATPase by S. Highsmith and D.J. Scales, University of the Pacific, San Francisco, CA 94115

CaATPase was specifically and stoichiometrically modified at the ATP binding site with fluorescein isothiocyanate (FITC) at pH 7.5. The fluorescence at 520 nm increased 12% due to added vanadate in the μM range, when Ca(2+) was absent and mM Mg(2+) was present, as in Pick and Karlish (1982, JBC 257, 6120). The apparent association constant was $K = 1 \times 10^6\ M^{-1}$ at pH 7 and 25°C.

Higher [vanadate] caused a 25% decrease in FITC-CaATPase fluorescence. $K = 380\ M^{-1}$ for this new low-affinity binding. The binding, as detected by the fluorescence decrease, was not sensitive to [Ca] or [Mg] between 10^{-8} and 10^{-3} M. The apparent low-affinity binding could be due to orthovanadate binding at a site different from the high-affinity binding site, or to an oligomeric vanadate (present in the high [vanadate] required) binding at the high-affinity site or at a different site. The low-affinity vanadate binding was reversible.

Vanadate-induced two-dimensional arrays of the CaATPase were prepared as described by Dux and Martonosi (1983, JBC 258, 1599). FITC-CaATPase and CaATPase formed identical 2D arrays, when the low-affinity vanadate binding was saturated. In both cases, mM Mg(2+) was required and Ca(2+) was inhibitory. When only the high-affinity vanadate binding was saturated, 2-D arrays were not observed.

The [Ca] dependencies of the high- and low-affinity vanadate binding and of array formation suggest that array formation requires either both high- and low-affinity binding, or that it is due to low-affinity binding of an oligomeric species of vanadate at the high-affinity binding site.

W-AM-F5 A FUNCTIONAL ROLE FOR DYNAMIC PROTEIN INTERACTIONS IN SARCOPLASMIC RETICULUM. Thomas C. Squier, Stephanie E. Hughes, and David D. Thomas. Dept. of Biochem., Univ. of MN, Mpls.,MN

We have investigated the functional role of the rotational mobility of the Ca-ATPase in sarcoplasmic reticulum. Saturation-transfer EPR (ST-EPR) was used to measure the overall rotational diffusion of the enzyme in order to (1) assess the importance of Brownian diffusion to the reaction mechanism and (2) to monitor changes in the degree of oligomerization in different enzymatic states.

First, we have demonstrated that ST-EPR measures overall rotational mobility (D_R), where $D_R \propto T/V\eta$, and not protein segmental flexibility. Second, increased enzymatic activity correlated with increased protein mobility in experiments involving protein cross-linking, partial delipidation, introduction of viscous solvents, and changes in temperature, suggesting a role for D_R. Third, similarities in Arrhenius slopes of enzymatic activity and protein rotational mobility suggest that protein diffusion is necessary for ADP-insensitive phosphoenzyme formation and may be rate-limiting under physiological conditions. Finally, equilibrium experiments suggest that conditions favoring phosphoenzyme formation favor protein association. This suggests a correlation between the oligomeric state and phosphoenzyme.

Since protein diffusion is important for the formation of ADP-insensitive phosphoenzyme (which has an apparant mass twice that of resting enzyme), changes in the oligomeric state of the Ca-ATPase may be important in the enzymatic cycle. We suggest that the formation of the ADP-insensitive phosphoenzyme involves the productive collision of monomeric forms of the Ca-ATPase, resulting in dimer formation.

W-AM-F6 LOSS OF MOTIONALLY RESTRICTED LIPID POPULATION CORRELATES WITH ACTIVATION OF THE CA-MG-ATPASE OF SARCOPLASMIC RETICULUM. Diana J. Bigelow and David D. Thomas, Dept. of Biochemistry, University of Minnesota, Minneapolis, MN 55455.

Lipid-protein interactions of activated Ca-ATPase were investigated by means of both conventional and saturation-transfer EPR of spin-labeled lipid and protein. A two-fold enzymatic activation, without increased vesicle permeability, results from the addition of 5% (v/v) diethyl ether to SR membranes. Spin-labeled phospholipid analogs report a progressive fluidization of the lipid hydrocarbon chains by increasing amounts of ether; **maximally**-activated membranes have the same average lipid chain mobility as does an aqueous dispersion of extracted SR lipids. The major effect of ether is to remove the spectral component corresponding to a fraction of motionally restricted, (possibly boundary lipid) chains. Quantitation of this restricted population by spectral subtractions indicates that this restricted fraction is 30% in the absence of ether and 0% in maximally-activated membranes. Overall rotational mobility of the enzyme, as measured by saturation-transfer EPR, increased two-fold, probably due to decreased protein-lipid and protein-protein interactions. Arrhenius plots of activity indicate that the formation of ADP-insensitive phosphoenzyme ceased to be rate-limiting in the presence of 5% diethyl ether. Loss of motionally-restricted lipid may activate by (1) facilitating either an overall or local conformational change (within the monomer) necessary for calcium transport or (2) increasing protein translational diffusion, thus allowing increased rates of protein association and dissociation necessary for calcium transport.

W-AM-F7 LOCALIZATION OF THE FUNCTIONAL SITES WITHIN THE TERTIARY STRUCTURE OF THE Ca-ATPase OF SARCOPLASMIC RETICULUM Terrence L. Scott, Dept. of Muscle Research, Boston Biomedical Research Institute, Boston, MA 02114.

The SR Ca-Mg ATPase has been labeled with both covalent and noncovalent probes at the Ca binding-transport sites (lanthanides, fluorescent carbodiimides (FCD)) and the nucleotide binding-hydrolytic site (TNP-nucleotides, fluorescein 5'-isothiocyanate (FITC)). Resonance energy transfer experiments indicate that the intramolecular distance between the Ca sites is < 15 Å while the Ca sites are 40-50 Å from the nucleotide site.

Energy transfer measurements under rapid diffusion conditions between donors and acceptors in which one is bound to the enzyme and the other free in solution have established that the FITC label in the nucleotide site is < 10 Å from the protein-aqueous interface.

These distances provide three-dimensional constraints on possible locations of the functional sites within the tertiary structure of the polypeptide. Supported by NIH Grant GM 32247.

W-AM-F8 IDENTIFICATION AND CHARACTERIZATION OF THE 53,000 Da AND 160,000 Da GLYCOPROTEINS AND THE Ca -ATPase OF SARCOPLASMIC RETICULUM IN RED AND WHITE SKELETAL, SMOOTH, AND CARDIAC MUSCLES. David R. Pepper, Carol Reynolds Raab and Kevin P. Campbell, Dept. of Physiology and Biophysics, The University of Iowa, Iowa City, IA 52242.

The distribution of the 53K Da and 160K Da glycoproteins and the Ca^{2+}-ATPase in isolated membranes from various muscles was determined using purified monoclonal antibodies directed against these proteins. Immunoblot analysis of the membrane vesicles from several red and white skeletal muscles, cardiac muscle, esophagus, stomach, intestine and the uterus has shown that 1) the presence of the 53K Da glycoprotein is always correlated with the presence of the 160K Da glycoprotein, 2) the molecular weight of each glycoprotein is identical in each membrane preparation and 3) the 53K Da and 160K Da glycoproteins are found in both light and heavy sarcoplasmic reticulum vesicles. All monoclonal antibodies directed against the 53K Da glycoprotein have been shown to react with the 160K Da glycoprotein, while the monoclonal antibodies directed against the 160K Da glycoprotein do not react with the 53K Da glycoprotein. Thus the 160K Da glycoprotein probably contains a region which is homologous to the 53K Da glycoprotein and a region which is different from the 53K Da glycoprotein. Immunoblot analysis has also indicated a relationship between the Ca^{2+}-ATPase and the 53K Da and 160K Da glycoproteins. Presence of the ATPase is always correlated with the presence of the 53K Da and 160K Da glycoproteins. Those membrane preparations with no detectable Ca^{2+}-ATPase were also negative for both glycoproteins. In addition, there appears to be a quantitative relationship between the 53K Da glycoprotein and the Ca^{2+}-ATPase which is currently being measured using a secondary ^{125}I-goat anti-mouse antibody. (Supported by NIH (NS 18814), MOD and MDA)

W-AM-F9 MONOCLONAL ANTIBODY LOCALIZATION OF 53,000 Da GLYCOPROTEIN AND Ca^{2+}-ATPase OF THE SARCOPLASMIC RETICULUM IN RABBIT SKELETAL MUSCLE. Barry Timms and Kevin P. Campbell (Intr. by Byron Schottelius) Dept. of Anatomy, and Dept. of Physiology and Biophysics, Univ. of Iowa, Iowa City, IA 52242

The ultrastructural localization of the 53K Da glycoprotein and Ca^{2+}-ATPase in rabbit skeletal muscle was determined by indirect immunogold labeling of longitudinal, ultrathin frozen sections. Purified monoclonal antibodies directed against the cytoplasmic portion of the 53K Da glycoprotein and the Ca^{2+}-ATPase were used for labeling. Ca^{2+}-ATPase was found to be distributed throughout the free sarcoplasmic reticulum. Examination of the qualitative localization of gold particles following staining for Ca^{2+}-ATPase demonstrated a close association with membranes of the longitudinal sarcoplasmic reticulum and non-junctional regions of the terminal cisternae. The 53K Da glycoprotein was also distributed throughout the free sarcoplasmic reticulum and found in similar regions to the Ca^{2+}-ATPase. Junctional sarcoplasmic reticulum, transverse tubules and myofibrils were only labeled at background levels. A significant proportion of the gold label following staining for the 53K Da glycoprotein was found associated with the terminal cisternae close to the 'Z' line. Small electron dense regions between the myofibrils, representing a portion of the fenestrated collar of free sarcoplasmic reticulum adjacent to the 'M' line, were occasionally associated with small clusters of gold particles following both Ca^{2+}-ATPase and glycoprotein staining. These results are consistent with our findings using isolated light and heavy sarcoplasmic reticulum vesicles and demonstrated that the 53K Da glycoprotein is found throughout the free sarcoplasmic reticulum like the Ca^{2+}-ATPase. (Supported by NIH (NS 18814), MOD and MDA)

W-AM-F10 VOLTAGE-DEPENDENCE OF PHOSPHOENZYME FORMATION OF RECONSTITUTED CA2+-ATPASE VESICLES. Boston University School of Medicine, Department of Physiology. Javier Navarro, Hae-Yung Pyun and Alvin Essig.

Ca^{2+}-ATPase was isolated by octylglucoside extraction of sarcoplasmic reticulum from rabbit skeletal muscle and reconstituted into egg phosphatidylcholine/cholesterol vesicles by the freeze-thaw sonication method. Proteoliposomes were further purified by sucrose gradient centrifugation. Steady state electrical potentials across the proteoliposome membranes were clamped by employing potassium gradients and valinomycin, and monitored with either voltage-sensitive dyes (e.g. di-O-C_2 [5]) or by determining the distribution of ^{14}C-TPP^+ (tetraphenylphosphonium). Our previous results indicated that negative electrical potentials enhance Ca^{2+} uptake whereas positive electrical potentials reduce Ca^{2+} uptake in proteoliposomes. Over a range of +50 mV to -100 mV, there was an inverse relationship between Ca^{2+} uptake and voltage (Biophysical J. December 1984). Determination of the phosphoenzyme intermediate in proteoliposomes were carried out at 0^oC. Negative electrical potentials increase the total amounts of phosphoenzyme whereas positive electrical potentials reduce the formation of the phosphoenzyme. Furthermore, the formation of ADP-sensitive phosphoenzyme was greatly enhanced by negative electrical potentials. On the other hand the level of the ADP-insensitive phospho enzyme was unaffected by voltage. Our findings suggest that the voltage affects specific steps of the Ca^{2+} pump cycle. (Supported by USPHS grant AM 27951 and Whitaker Health Sciences Fund Grant).

W-AM-F11 ANALYSIS ON BASIS OF Ba EFFECTS ON THE FROG MUCOSA OF A GASTRIC PROTON PUMP MODEL INCORPORATING A NEUTRAL K-H ATPase PUMP. W. S. Rehm, G. Carrasquer, and M. Schwartz, Depts. of Medicine and Physics, University of Louisville, Louisville, KY 40292.

According to Forte's and Sach's groups the gastric K-H ATPase pump is neutral. Both groups use a model for the intact mucosa in which KCl enters the lumen via conductive pathways and K is exchanged for H resulting in HCl secretion. The model will be analyzed on the basis of effects of Ba on the frog gastric mucosa. In secreting in-vitro frog gastric mucosa, with 4 mM K on each side, Ba (1 mM) added to the nutrient (serosal) (N) produces a marked increase in resistance while when added to secretory (S) (up to 25 mM) has little effect. Ba added on either side did not affect H secretion. The acid rate is not changed upon removal of K from S with 4 mM K in N. With 4 mM K in S, removal of K from N reduces acid rate to 40% and then acid rate to zero upon removal of K from S. With 0 K in N and 4 mM K in S, Ba (2 mM) added to S reduces acid rate to zero. With Ba still present on S, high concentrations of K (20 mM) to this side restores the acid rate in about 1 minute. Substantial evidence supports concept that Ba blocks K conductance channels. Therefore, under standard secretory conditions with Ba on S (2 to 25 mM), K cannot move from cell to lumen. As a consequence, Cl can then not move from cell to lumen and hence the movement of KCl from cell to lumen is not essential for acid secretion. Furthermore, with 4 mM K in S and zero K in N, and with K channel on S blocked by Ba, the acid rate should still continue due to 4 K on S if there is a K-H exchange at the lumen-cell interface. However, H rate goes to zero. It is concluded that the above model is not viable. (NSF and NIH support)

W-AM-F12 RECONSTITUTION OF THE FUNCTIONAL GASTRIC [H,K]-ATPase
E Rabon, R Gunther, S Bassilian and G Sachs, CURE/VA Wadsworth and UCLA, Los Angeles, CA 90073

The transport reactions of the hog gastric [H,K]-ATPase have been reconstituted from cholate and n-octylglucoside solubilized membranes using F/T/S and/or detergent dilution techniques. Purification of the reconstituted material by sucrose density gradient centrifugation provided two ATPase containing fractions, only the lighter of which showed ATP and K dependent proton transport. Compared to native membranes, the sucrose gradient resolved material was 2 fold enriched in steady-state phosphoenzyme and ATPase activity. In contrast to the several peptides seen in the native material, only a single 94 kdalton peptide was found after SDS PAGE. Cation transport was studied using ^{86}Rb uptake into cation loaded vesicles. The selectivity of uptake was K=Rb ⟩ Na ⟩ Li. Na or Li preloaded vesicles but not TMA preloaded vesicles showed MgATP dependent intravesicular acidification when diluted into K media. This demonstrated the identity of the vesicles containing the cation and proton transporter. Uptake had a saturable and non-saturable component with a $K_{0.5}$ of 1.6 mM. In contrast to the hydrolytic cycle, Rb/Rb exchange did not exhibit a clear pH dependent shift in $K_{0.5}$. No ligand stimulation of the saturable component was found, but vanadate, omeprazole and other ATPase ligands were found to be inhibitory. Thus this cation pathway appears to be a property of the catalytic subunit of the ATPase and dependent on both the E1 and E2 conformers. A measured equality of the MgATP dependent Rb efflux and Rb/Rb exchange rates suggested that the gastric enzyme may not have an occluded K form. (Supported by NIH grant AM 34286-01, and the Veterans Administration).

W-AM-G1 LIGHT CHAIN INTERACTIONS IN SKELETAL MUSCLE MYOSIN AND MYOSIN SUBFRAGMENT 1. S.C. Pastra-Landis and Susan Lowey. Wheaton College, Norton, MA 02766 and Rosenstiel Center, Brandeis University, Waltham, MA 02254.

The alkali light chains (LC1 and LC3) of chymotryptic myosin subfragment 1 (S1) dissociate reversibly at 37°C in 10 mM MgATP (Sivaramakrishnan and Burke, 1981). In contrast, these alkali light chains do not exchange in the intact myosin species or the light-chain homodimers (Waller and Lowey, 1983). Since the 20K dalton light chain (LC2) is absent in chymotryptic S1, a possible role for the LC2 has been postulated. Chicken pectoralis skeletal myosin entirely denuded of LC2 can be prepared (Pastra-Landis and Lowey, 1984) by immunoaffinity chromatography at 37°C, using a polyclonal antibody specific for LC2. The availability of this material makes it possible to investigate the function of the LC2 in the strength of binding of LC1 and LC3 to heavy chains. Alkali light chain exchange was studied using LC2-deficient myosin with a 10-fold molar excess of LC1. Hybrid formation was detected by electrophoresis in a non-denaturing pyrophosphate buffer on polyacrylamide gels. Under these conditions, pure LC1 homodimer of the myosin was formed at 37°C, demonstrating complete exchange, while no exchange occurred at 4° or 25°C. Papain subfragment 1, which retains the LC2, showed no alkali light chain exchange with 10-fold molar excess of LC1. We conclude that the interaction of the alkali light chain subunits with the heavy chain is directly dependent on the presence of the 20K dalton LC2, which must have an important stabilizing role. In the absence of the LC2, the alkali light chains can exist in a dynamic equilibrium at elevated temperatures, whether they are bound to the intact heavy chain of the myosin molecule or to the heavy chain of subfragment 1. (Supported by grants from NIH, NSF, and MDA to S.L.).

W-AM-G2 MODIFICATION OF RABBIT MYOSIN SUBFRAGMENT ONE (S-1) WITH THE TRYPTOPHAN-SELECTIVE REAGENT, DIMETHYL (2-HYDROXY 5-NITROBENZYL) SULFONIUM BROMIDE (DHNBS), Moshe M. Werber[1] and A. Muhlrad[2], [1]Department of Medical Laboratories, Meir Hospital, Kfar-Sava and [2]Department of Oral Biology, Hebrew University-Hadassah Faculty of Dental Medicine, Jerusalem, Israel.

Modification of tryptophanyl(Trp) residues of myosin S-1 was performed using DHNBS. Under controlled conditions, pH 6 at 0° and 10 min reaction with 20-170-fold molar excess of DHNBS, between one and eight 2-hydroxy 5-nitrobenzyl (HNB) residues were incorporated in S-1. Concomitant with the modification at a 160-fold molar excess, EDTA-ATPase activity was reduced to 40% whereas Ca-ATPase activity was slightly increased. A 40% decrease in the effect of CaATP and MgATP on the intrinsic fluorescence of S-1 was also observed. The modification of as few as 1-2 Trp residues caused a blue shift of the emission spectrum, accompanied by a 30% reduction in the fluorescence quantum yield. The number of modified Trp residues was determined by fluorescence of the denatured samples (either in SDS or guanidinium hydrochloride). Up to a 50-fold molar excess of DHNBS, the number of modified Trp agreed well with the number of HNB residues incorporated in S-1. Under these conditions the thiol groups of S-1 were found to be unaffected, thus indicating that the modification was selective for Trp residues. Recently, a Trp residue was identified in a photoaffinity-labeled active site peptide (Y. Okamoto and R.G. Yount, Biophys. J. 41, 298a, 1983). Under our very mild experimental conditions, this may be the first Trp residue that DHNBS modifies.
Supported by the Israel-US Binational Science Foundation.

W-AM-G3 THE EFFECT OF TRYPTIC CLEAVAGE ON THE STABILITY OF THE SUBUNIT INTERACTIONS IN MYOSIN SF1. Morris Burke, James Craig and Bruce Mathern, Department of Biology, Case Western Reserve University, Cleveland, OH 44106.

It has recently been demonstrated that tryptic cleavage of SF1(A2) which is confined to two regions of the heavy chain subunit located at about 27K and 75K from the amino-terminus markedly destabilizes the subunit interactions of this protein (Burke and Kamalakannan. Biochemistry (1984, in press)). In the present study we have sought to determine whether this destabilization requires cleavages at both sites or if cleavage at just one of these sites is sufficient. Tryptic SF1(A2) species with cleavage at either of the two protease-sensitive sites have been subjected to thermal ion-exchange chromatography and the extent of subunit dissociation induced by this procedure has been determined for both of these species. The results obtained indicate that tryptic cleavage at either of these two sites alone does not significantly destabilize the interaction between the two subunits and, therefore, the destabilization noted previously does require cleavages at both sites in the heavy chain subunit. Additionally, the isolated severed heavy chains of these tryptic SF1 species have been examined for their ATPase properties in the presence and absence of actin. It is found that these heavy chains resemble closely their SF1 counterparts in this respect. Reassociation studies show that both forms of the severed heavy chain can rebind free A1 or A2 light chains to reconstitute the corresponding tryptic SF1 isozyme.
Supported by US Public Health Grant NS 15319.

W-AM-G4 AN INTACT 73K DOMAIN IS NECESSARY FOR THE HIGH SALT·ATPASE ACTIVITY OF SCALLOP S1.
E. M. Szentkiralyi, Department of Biology, Brandeis University, Waltham, Massachusetts 02254.

The functions of the large polypetide chain of subfragment 1 (S1) can be assigned by limited proteolysis. Trypsin cleaves scallop S1 at proteolytic site A into a C-terminal 24K and an N-terminal 73K fragment. This is similar to the action of trypsin on vertebrate S1s. Such nicked S1 retains ATPase activity in 0.5M KCl in presence or absence of divalent cations but loses actin activation. The 73K peptide is labile and is fragmented further through a 63K intermediate, severed at proteolytic site B, into smaller peptides. As described earlier (Szentkiralyi, Journal of Muscle Research and Cell Motility, 5, 147, 1984) a more stable nicked S1 was made by digesting S1 bound to actin; site A was protected and nicked S1 consisting of a C-terminal 31K and an N-terminal 63K peptide was produced. S1 heavy chain (HC) concentration declined parallel with the loss of ATPase activity in high salt during digestion. If S1 was digested in the absence of actin the high salt ATPase was proportional to the sum of S1 HC + 73K fragment. I conclude that a nicked S1 having the 63K peptide as an N-terminus lacks ATPase activity. It is possible that the 63K-31K junction, near both actin binding sites, but far removed from the nucleotide binding site, contributes to the active site either directly or indirectly. (Supported by NIH AM-15963 and MDA grants)

W-AM-G5 INTER-HEAD FLUORESCENCE ENERGY TRANSFER BETWEEN PROBES IN SCALLOP MYOSIN.
Peter D. Chantler & Terence Tao. Medical College of Pennsylvania, Philadelphia,PA. 19129 and Boston Biomedical Research Institute, Boston, MA. 02114.

The biphasic reuptake of regulatory light-chains (R-LCs) by 35°-desensitized scallop myofibrils (Chantler & Szent-Györgyi, 1980. J.Mol.Biol. 138. 473) makes it possible to carry out energy transfer measurements between translationally equivalent sites on each head of a single myosin molecule. R-LCs, possessing either one (Mercenaria, chicken gizzard) or two (Loligo, rabbit skeletal) SH groups were modified with 1,5-IAEDANS or DABMI (4-dimethylamino-phenylazophenyl-4'-maleimide) as energy transfer donor or acceptor, respectively. The modified R-LCs were added to desensitized scallop myofibrils, ultimately yielding fully active hybrid myosin molecules. In all cases studied, energy transfer efficiencies (measured by either steady-state or lifetime techniques) of no more than 5% were obtained, indicating that the inter-head R-LC SH sites are at least 65 Å apart. Photochemical crosslinking studies have shown that the SH group of the Mercenaria R-LC on one head is $\leqq$9 Å from the region of closest approach of the R-LC on the other head (Hardwicke & Szent-Györgyi, 1984. Biophys.J. 45. 229a). Taken together, these two studies suggest a topology for the myosin molecule in which this region of closest approach, within the R-LC on the second head, is considerably distant from R-LC residue number 50 (the approximate location of the SH residue in Mercenaria R-LC) and are consistent with an inbuilt asymmetry which relates the two heads of the myosin molecule.
Supported by Grant No. AM 32858 (P.D.C.) and Grant No. AM 21673 (T.T.). P.D.C. is an Established Investigator of the American Heart Association.

W-AM-G6 STRUCTURAL CHARACTERIZATION AND ACTIN INTERACTION OF ISOLATED RENATURED FRAGMENTS OF MYOSIN S-1.
Andras Muhlrad, Kathleen Ue & Andrzej Kaspzrak. CVRI, U. of Calif., San Francisco CA 94143.

This is an extension of our recent studies [Muhlrad & Morales 1984 PNAS 81:1003-1007) on isolation and characterization of partially renatured 20 kDa and 50 kDa tryptic fragments of S-1 heavy chain. Here we show the CD spectrum of denaturant-free 50 kDa fragment; it indicates at least partial refolding. The Trp emission spectrum of 50 kDa closely resembles that of intact S-1. The 3 Trps of 50 kDa are evidently partially buried as they are only slightly quenched by acrylamide. Torgerson (Biochemistry 23:3002-3007, 1984) established 3 lifetime classes in S-1; the Trps of 50 kDa fall approximately into the same classes; however, the fraction having longest lifetime is much less than in S-1. Isolated 50 kDa slightly inhibits the actin activated ATPase of S-1, while 20 kDa strongly inhibits the same activity. However, the actin inhibition of the K^+(EDTA)-activated S-1 ATPase is not affected by 20 kDa. 20 kDa is cross-linked to actin by 1-ethyl-3-(3-dimethylaminopropyl) carbodiimide and inhibits the formation of cross-links between actin and tryptically-cut S-1 both at 20K and 50K sites. When 1,5-AEDANS-labelled F-actin is overlaid on SDS-PAGE of tryptically-split S-1 that has later been rid of denaturant, it binds much more strongly to 20 kDa than to 50 kDa. The foregoing points to the existence of domain structure in S-1. Support from AHA, NHBLI, NSF and BSF are gratefully acknowledged.

W-AM-G7 INTERNAL MOTIONS IN MYOSIN ROD MEASURED BY SOLID STATE CARBON-13 NMR

T. M. Eads, S. Ganapathy, V. P. Chacko, & R. G. Bryant, Radiology Department, Box 648, University of Rochester Medical Center, Rochester, New York 14642

As a step toward describing contractile events in terms of internal motions, we used solid state NMR to estimate amplitudes and rates of backbone atom motion in filaments (u=0.1) and monomers (u=0.6) of myosin rod, a two-stranded coil of alpha helices, M_r=220,000. Natural abundance carbon-13 spectra obtained with strong proton decoupling showed a carbonyl lineshape dominated by the chemical shift interaction, partially narrowed by backbone motion in the kilohertz range to less than half the rigid limit value. Narrowing was greater in monomers. Monomeric rod also contains very mobile backbone atoms (MHz range) (Eads & Mandelkern (1984) J. Biol. Chem. 259, 10689). Filament spectra obtained with varying cross polarization (^1H-^{13}C) contact time allow selective observation of different motional classes of backbone and sidechain atoms. Carbonyl CP lineshape was thus used to monitor motional frequencies with changes in temperature and ionic strength. A comparison was made between observed and simulated spectra incorporating effects of motional averaging of the chemical shift tensor. Ranges in motional frequency and amplitude were obtained, reporting motions in a range not previously observed in rod. These direct results will be compared to results of other measures of flexibility in rod. (Supported by NIH grants GM-29428 and GM-34541.)

W-AM-G8 AXIAL ARRANGEMENT OF THE MYOSIN ROD IN VERTEBRATE THICK FILAMENTS: IMMUNOELECTRON MICROSCOPY WITH A MONOCLONAL ANTIBODY TO LIGHT MEROMYOSIN. T. Shimizu, J.E. Dennis, T. Masaki, and D.A. Fischman, Department of Cell Biology and Anatomy, Cornell University Medical College, New York, NY 10021.

A monoclonal antibody (McAb), MF20, has been proven to bind the light meromyosin (LMM) fragment of purified myosin. Epitope mapping by E.M. of rotary-shadowed, myosin-antibody complexes, has localized the binding site to the rostral portion of LMM, ∿76nm from the tip of the myosin tail. Since this epitope is accessible to McAbs, we used the McAb to analyse the packing of LMM along the thick filament backbone. By immunofluorescence, MF20 was shown to bind the entire A-band of chicken myofibrils, although the epitope accessibility was greater near the ends than the centers of the A-bands. Thin-section, transmission E.M. of myofibrils decorated with MF20 revealed 50 regularly spaced, cross-striations in each half A-band (repeat distance 12-13nm). These same striations were visualized by negative staining of thick filaments labeled with MF20. All 50 striations were of a consecutive, uninterrupted repeat approximating the 14-15nm axial translation of crossbridges. Each half M-region contained 5 MF20 striations (14-15nm apart) with a distance between stripes 1 and 1', on each half of the bare zone, of 16nm, compatible with a packing model of full, antiparallel overlap of myosin rods in the bare zone region. Differences in the spacings measured with negatively stained myofilaments and thin sectioned myofibrils have been shown to arise from specimen shrinkage in the embedded preparations. These results provide support for Huxley's proposal (1963) for myosin packing in thick filaments of vertebrate muscle and, for the first time, directly demonstrate that the 14-15nm axial translation of LMM in the thick filament backbone corresponds to the crossbridge repeat detected with X-ray diffraction of living muscle.

W-AM-G9 CROSSBRIDGE CONFIGURATION IN RELAXED FISH AND FROG MUSCLES. Jeff Harford, Marie Cantino* and John Squire, Blackett Laboratory, Imperial College, London and *Centre for Bioengineering, WD-12, Seattle, Washington.

X-ray diffraction studies have confirmed the prediction from electron microscopy (Luther et al, 1981, J.Mol.Biol. 151, 703) that the myosin filaments in relaxed bony fish muscles form a crystalline array. This contrasts with higher vertebrates where there is an A-band superlattice with statistical disorder (Luther & Squire, 1980, J.Mol.Biol. 141, 409) and with insect flight muscles where there is a nearly random distribution of A-filaments among three possible filament orientations (Freundlich & Squire, 1983, J.Mol.Biol. 169, 439). In both cases, the disorder makes difficult the determination from X-ray data of the crossbridge configuration in relaxed muscle. However, the intensities in the 'crystalline' X-ray patterns from relaxed fish muscle (plaice fin) can be satisfactorily modelled to give a good fit (R factor ~0.3) if the two myosin heads on each lattice point are tilted 0-30° from normal to the myosin filament axis and slewed 0-30° from a radial direction through the crossbridge origin. Separate studies of myosin filament images in shadowed replicas of freeze-fracture surfaces of relaxed frog semitendinosus fibres frozen using dual propane jet freezing device, (Cantino & Pollack, 1983, Biophys.J.I, 264a) have revealed that here the myosin heads probably have a similar configuration on the right-handed helical strands to those in fish except for a larger tilt (60-70°). This tilt puts the myosin heads at a smaller radius than in fish, consistent with X-ray layer line patterns from frog. Thus there is a good correlation between the two results. Attempts are now being made to assess whether fish muscle is suitable for time-resolved X-ray diffraction studies: any observed changes could in this case be related to a known starting structure in relaxed fish muscle.

W-AM-G10 SUBFILAMENT STRUCTURE OF TUBULAR FILAMENTS OF INSECT FLIGHT MUSCLES. Gernot Beinbrech, Francis T. Ashton and Frank A. Pepe, Zoologisches Institut, D4400 Munster, FRG, and Dept. of Anatomy, Univ. of Pennsylvania, Philadelphia, PA 19104.

Cross sections (100-140 nm thick) of the flight muscles of the fleshfly Phormia terrae-novae and the housefly Musca domestica (fixation procedure 3 of Ashton and Pepe, J. Microsc. 123:93-104, 1981) were photographed in a JEM-200 A electron microscope. The images of 52 tubular filaments of the fleshfly and 67 filaments of the housefly were digitized and computer processed by rotational averaging (Stewart et al., J. Mol. Biol. 153:381-392, 1981). The rotational power spectra of about 80% of the filaments showed peaks for six fold rotational frequency. Images rotationally averaged by using the 6 fold components of the power spectrum could be categorized into several groups. The characteristic pattern consisted of 12 subunits arranged in 6 pairs which were separated by gaps. This arrangement was also obtained when the electron micrographs of all filaments were superimposed. The angle required to bring the images into phase was determined from the filtered images of the individual filaments. The center to center distances of the subunits were 2.8 nm within one pair and 4 nm between two neighboring subunits at either side of the gap. Assuming a 4-stranded cross-bridge arrangement we concluded that each subunit represents a subfilament. The cross section of a subfilament transects two LMM and one S2 portion of myosin at any particular level along the filament axis (i.e. the subfilament is made up of myosin molecules with a 43 nm stagger between the molecules).

W-AM-G11 SUBFILAMENT STRUCTURE OF MYOSIN FILAMENTS IN THE LOBSTER FAST DEEP EXTENSOR MUSCLE. Francis T. Ashton, Gernot Beinbrech and Frank A. Pepe, Dept. of Anatomy, Univ. of Pennsylvania, Philadelphia, PA 19104 and Zoologisches Institut, D4400 Munster, FRG.

The muscle was fixed by the multistage fixation procedure previously shown to preserve subfilament organization in vertebrate skeletal myosin filaments (Ashton and Pepe, J. Microsco. 123:93-104, 1981). Transverse images of the myosin filaments were obtained from sections 80-140nm thick. The images of 82 filaments were digitized and computer processed by rotational averaging (Stewart et al. J. Mol. Biol. 153:381-392, 1981). The rotational power spectra of about 75% of the filaments showed peaks for six fold rotational frequency. Images rotationally averaged by using the 6 fold components of the power spectrum, characteristically consisted of the pattern of 2 subunits arranged in six pairs which is also observed with insect flight muscles (see abstract by Beinbrech, Ashton and Pepe). However, in the lobster filaments additional asymmetrically located subfilaments were observed inside the cylindrically arranged peripheral ones. Although in some instances the position of these subfilaments appeared to change in serial sections along the same filament, no clear pattern of change was observed. With sections 140nm thick, a tilt series of images differing in tilt by 2^{o} was taken for the same filament. The effect on the image of tilting by 2^{o} was that the individual subfilaments became elongated in the direction of tilt as expected for subfilaments essentially parallel to the long axis of the filament. We conclude from these observations that the cylindrical elements in the lobster muscles are structurally similar to those in the insect flight muscle. However, the lobster filaments contain core subfilaments which are asymmetrically located and which possibly may be related to paramyosin.

W-AM-G12 ARCHITECTURE OF THE TITIN/NEBULIN CONTAINING CYTOSKELETAL LATTICE OF THE STRIATED MUSCLE SARCOMERE -- EVIDENCE OF ELASTIC AND INELASTIC DOMAINS OF THE BIPOLAR FILAMENTS. K. Wang, J. Wright, R. Ramirez-Mitchell, Clayton Foundation Biochemical Institute, Department of Chemistry, and Cell Research Institute, The University of Texas, Austin, Texas 78712.

We have prepared a library of monoclonal antibodies directed to four distinct epitopes of rabbit titin and utilized fluorescent techniques and colloidal gold electron microscopy techniques to study the disposition of these distinct epitopes in the sarcomere. We observed that each of four monoclonal antibodies stained a pair of distinct transverse bands within either the A band or the I band. Furthermore, each pair of bands were centered at the M line. These staining data confirmed our earlier conclusion that titin domains are indeed wider than the A band (K. Wang in Contractile Mechanisms in Muscle, 1984, Plenum Press:285). It can be inferred that titin-containing filaments are centrally symmetric to the M line, and that these parallel longitudinal filaments are aligned transversely within the sarcomere. Furthermore, we observed that the axial disposition of some, but not all, epitopes varied with the sarcomere length. The epitopes within the I band exhibited an elastic stretch-dependence; whereas those within the A band remained fixed in position. These data suggest that in intact sarcomeres, the elastic cytoskeletal filaments are stretchable only in the I band domain. The filament domains within the A band may be prevented from stretching by certain as yet undefined anchoring mechanisms. Supported in part by NIH AM20270, American Heart Association, Texas Affiliate, and an American Heart Association Established Investigatorship.

W-AM-H1 EXISTENCE OF HUMP CHARGE COMPONENT IN FROG SLOW MUSCLE FIBERS. Chiu Shuen Hui. Dept. of Physiol. and Biophys., Indiana University Medical School, Indianapolis, IN 46223, USA.

Charge movement recorded from frog twitch fibers bathed in a moderately hypertonic solution consists of a main component and a hump component (Hui, J. Physiol. **337**: 509, 1983). The latter component appears to be closely associated with calcium release from the sarcoplasmic reticulum (SR). Similar experiments were performed on slow fibers in pyriformis muscle of warm-adapted *Rana temporaria*. The techniques for dissection and fiber identification were modified from those used by Gilly and Hui (J. Physiol. **301**: 137, 1980). Charge movement traces were signal-averaged heavily to improve signal-to-noise ratio. It was found that the hump charge component also exists in slow fibers in the same potential range as in twitch fibers. More importantly, the time-course of the hump component in slow fibers is similar to that in twitch fibers. If the time-course of the rise in myoplasmic calcium level in slow fibers is much slower than that in twitch fibers (Miledi, Parker and Schalow, Nature **268**: 750, 1977), this would rule out the possibility that the hump component is a consequence of calcium release from the SR.

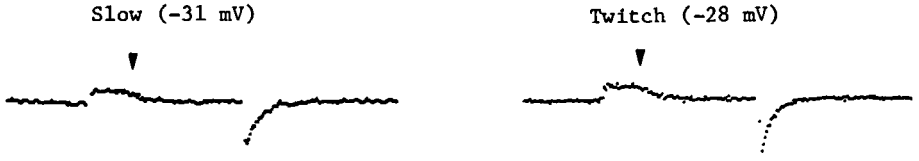

W-AM-H2 VOLTAGE DEPENDENT CHARGE MOVEMENT AND BARIUM CURRENT IN INVERTEBRATE SKELETAL MUSCLE. T. Scheuer & W.F. Gilly, Hopkins Marine Station of Stanford University, Pacific Grove, CA 93950

Voltage clamp experiments were carried out on striated muscle of the scorpion (Centuroides sculpturatus) to determine whether charge movement signals resembling those found in vertebrate skeletal muscle could be detected. Scorpion muscle has a fast, voltage dependent calcium conductance and E-C Coupling is abolished in Ca-free media (Gilly & Scheuer, 1984; J.G.P. 84, 321-345. A standard 3-microelectrode voltage clamp method was used at the ends of muscle fibers (Schneider & Chandler, 1976; J.G.P. 67, 125-163). For charge movement experiments, ionic currents and contraction were blocked by replacing Na in the bathing medium with tetraethylammonium ions and by replacing Ca with Mg. 1-5 mM Ba was added for recording Ba currents. Fibers were held at -70 mV, and test depolarizations were compared to control pulses obtained from a hyperpolarizing well. Under these conditions (6-12^{o} C) depolarizations beyond -40 mV elicit a slow, voltage dependent component of capacity current. Amounts of charge moved during and after a pulse are approximately equal for pulse durations briefer than 50 ms. The relation between charge moved and voltage is sigmoidal and saturates near 0 mV; maximum moveable charge is about 10 nCoul/μF of membrane capacity. Longer pulses apparently immobilize the charge, and the ratio of charge moved during to after the pulse becomes greater than unity. The kinetics and voltage dependnece of Ba current activation and the time course of inactivation are all very similar to the analagous propetties of charge movement. These common features suggest that charge movement in scorpion muscle may be a Ca channel gating current.

W-AM-H3 ANTIPYRYLAZO III CALCIUM TRANSIENTS IN CUT FROG TWITCH FIBERS. M. Irving, W.K. Chandler, J. Maylie and N.L. Sizto. Department of Physiology, Yale University, New Haven, CT 06510. Fibers were mounted in a double gap chamber, 15 °C, which allows voltage recording and current passing (Kovacs, Rios & Schneider, 1983). A spot of 'white' light was focused on the fiber and transmitted light was separated into 3 different wavelengths, allowing simultaneous measurement of intensities. Dye-related absorbance at 550 nm, A(550), was used to estimate [dye], and dye-related ΔA(720) was used to monitor the action potential-induced Ca transient. 2-3 hours after addition of 0.25-0.5 mM dye to the end pools, [dye] at the optical site reached at least twice that in the end pools. Solution of the equation for diffusion, which includes absorption of dye in direct proportion to free [dye], gives on average a value of 1/3 for the ratio free:total dye. When dye was diffusing into a fiber, the peak of dye-related ΔA(720) followed a parabolic relationship with respect to total [dye] up to 0.3-0.5 mM, as expected for 1:2 stoichiometry of Ca:dye complex and constant free Ca. According to the calibrations of Rios & Schneider (1981) peak free Ca would be 2-3 μM if both bound and free dye participate equally well in complexing Ca. If only free dye (estimated as 1/3 of total dye) participates, peak free Ca would be 15-25 μM. Interestingly, the rate of decay of the Ca transient always decreased during the time course of an experiment. This occured whether [dye] was increasing, following end pool application, or was decreasing, following end pool removal. A possible explanation is that the internal environment in cut fibers changes with time, and that this could either slow the turn-off of calcium release following an action potential or decrease the rate of subsequent removal of myoplasmic free Ca.

W-AM-H4 LATE ANTIPYRYLAZO III SIGNALS IN CUT MUSCLE FIBERS. J. Maylie, W.K. Chandler, M. Irving and N.L. Sizto. Department of Physiology, Yale University, New Haven, CT 06510. In intact fibers containing AP III, an action potential produces a Ca transient which is followed by a maintained dye-related absorbance change. This late signal has a wavelength dependence that matches cuvette difference spectra for a small increase in either pH or Mg (Baylor, Chandler & Marshall, 1982). Cut fibers, studied at 15 °C (see preceding abstract), also have a maintained signal with similar spectral properties. The time dependence of this signal is best studied at 590 nm, an isosbestic wavelength for Ca. Repetitive stimulation at 100 Hz produces Ca signals of approximately constant peak but ΔA(590) signals which summate. Similarly, during 100-200 ms voltage steps the ΔA(590) signal continues to increase in cases where the Ca signal is nearly constant. During either action potential stimulation or voltage clamp, the ΔA(590) signal increases only during the time when free [Ca] is elevated and, in general, dΔA(590)/dt appears to be correlated with free [Ca]. These findings suggest that the ΔA(590) signal is a consequence of free [Ca]. After stimulation ΔA(590) signals decay towards baseline with a half time of 1-2 sec. Absorbance measurements were also carried out with the pH indicators phenol red and dimethylcarboxyfluorescein. Both indicators showed an early increase in pH, which lagged the retardation (and therefore Ca) signal, followed by a decay towards baseline. The pH signals decayed more rapidly, by an order of magnitude, than the AP III ΔA(590) signal. This suggests that the ΔA(590) signal cannot be explained entirely on the basis of an increase in pH.

W-AM-H5 OPTICAL STUDIES ON CUT MUSCLE FIBERS USING THE CALCIUM INDICATOR TETRAMETHYLMUREXIDE. J. Maylie, G. Boyarsky, W.K. Chandler, M. Irving and N.L. Sizto. Department of Physiology, Yale University, New Haven, CT 06510. Fibers were studied (see preceding abstract) using TMX which is sensitive to Ca but not to pH or Mg. The time course of dye diffusion both into and out of the fiber was well fitted by the equation for diffusion plus absorption. On average, the ratio free:total dye was 0.7 and the diffusion constant was $1.8 \times 10^{-6} cm^2/sec$ (15 °C), a value close to that obtained in skinned fibers for sucrose, which has a similar molecular weight (Kushmerick & Podolsky, 1969). The resting spectrum of dye-related absorbance, when compared with cuvette calibration spectra, indicates that approximately 20% of the dye is complexed with Ca (which would give a ratio free:total dye of 0.8). Since resting myoplasmic free Ca is less than 1 μM, the results indicate that at least 20% of the dye appears to be in a high-Ca environment such as inside the sarcoplasmic reticulum. Changes in dye-related absorbance following an action potential show the same waveform at different wavelengths, with amplitudes which match a cuvette Ca difference spectrum. The waveform shows an early increase in free Ca followed by a decrease, most likely due to dissociation of resting Ca:dye complex. The early peak dye-related ΔA(570) is a linear function of [dye], as expected for a Ca:dye stoichiometry of 1:1 and constant free Ca. The value of peak free Ca obtained with TMX is approximately 20 μM as compared with 2-3 μM obtained with Antipyrylazo III (preceding abstract). Calculations using model 2 (Baylor, Chandler & Marshall, 1983) indicate that less than 0.5 of the Ca-regulatory sites on troponin become occupied if 2-3 μM if used for peak Ca whereas 0.9 become occupied if 20 μM is used.

W-AM-H6 INOSITOL TRISPHOSPHATE INDUCED CONTRACTURES IN FROG SKELETAL MUSCLE FIBERS.
J. Vergara and R.Y. Tsien, Dept. of Physiology,UCLA and Dept. of Physiology-Anatomy,UC Berkeley.

Inositol 1,4,5 trisphosphate (IP_3) has been recently reported to act as a mediator in the release of calcium from endoplasmic reticulum in several preparations. We have investigated its ability to release calcium from the sarcoplasmic reticulum in frog skeletal muscle fibers and have found that it is effective at doses as low as 10 uM. Three types of experiments have been performed: a) IP_3 was delivered by pressure microinjection or microiontophoresis to mechanically skinned muscle fibers under oil immersion. Contractions were visualized with a compound microscope. b) Small volumes (nanoliters) of IP_3 containing solutions were delivered to short segments of mechanically skinned muscle fibers under oil immersion. Isometric tension was detected with a highly sensitive tension transducer. c) Short segments of muscle fibers mechanically skinned in aqueous relaxing solutions were mounted in a small volume chamber in which rapid changes of solutions of various IP_3 concentrations could be made. Tension was measured as above. The main observation was that IP_3 is able to produce contractions under each of the above conditions. Control experiments showed that these contractions were not due to direct effects of IP_3 on the contractile machinery. In addition, we observed that low free Mg concentrations and mM concentrations of 2,3 Diphospho-D-glycerate, both methods known to inhibit IP_3 breakdown, result in an increased effectiveness of IP_3. Our results suggest the possibility that IP_3 may be a natural internal messenger responsible for the Ca release from the sarcoplasmic reticulum in skeletal muscle fibers. We thank Dr. C. Ballou for his gift of IP_3 and other phosphoinositides. Supported by grants from USPHS (AM 25201) and MDA.

W-AM-H7 EFFECTS OF NEOMYCIN UPON CALCIUM RELEASE IN SKELETAL MUSCLE FIBERS, STUDIED WITH CALCIUM-SENSITIVE DYES. M. Delay, J. Vergara and R.Y. Tsien. Dept. of Physiology, UCLA, and Dept. of Physiology-Anatomy, UC Berkeley.

Internal solutions containing neomycin, at concentrations between 0.1 and 5 mM, as well as the metallochromic indicator dye Arsenazo III, were diffused into the interior of cut frog skeletal muscle fibers voltage-clamped using the triple vaseline gap technique. The presence of neomycin between 0.1 and 1 mM in the end pools resulted in a graded reduction of the Ca signal amplitude, between 0% at 1 mM and about 60% at 0.1 mM. The amplitude, time course and voltage dependence ot the Na and K currents were preserved over this range of concentrations. The time course of the Ca signals was not changed despite partial blockage of the Ca release in the presence of 0.1 and 0.5 mM neomycin, nor did these levels greatly alter the voltage dependence of the Ca signal amplitude. This inhibition of the Ca release by neomycin is partially reversed by high (5 mM) external concentrations of caffeine. The concentrations of neomycin used here are more than one order of magnitude lower than those reported to reduce Ca transport in other muscle preparations. However, these concentrations are within the range of those reported to inhibit polyphosphoinositide turnover in other preparations (Schacht, J. Neurochem. 27:1119 (1976)).

Supported by grants from USPHS (AM25201), MDA and a fellowship from AHA-GLAA.

W-AM-H8 CALCIUM TRANSIENTS IN FROG SKELETAL MUSCLE FIBERS INJECTED WITH AZO1. S. Hollingworth and S. M. Baylor. Department of Physiology, University of Pennsylvania.

The calcium indicator dyes Antipyrylazo III (Ap III) and Arsenazo III (Az III) have been used extensively to study myoplasmic free Ca transients during activity. There are difficulties, however, in interpreting signals from these dyes due both to their sensitivities to Mg and H and, in the case of Az III, to the formation of more than a single Ca-dye complex. In addition, all Ca-indicator dyes used intracellularly in muscle have, to date, shown evidence of dichroic component(s) of the absorbance signals. Recently, a new family of "tetracarboxylate" Ca-indicators with 1:1 Ca:dye stoichiometry and a high selectivity over Mg and H has been developed by R. Y. Tsien (Biochemistry 19, 2396-2404). We have used one of these dyes, Azo1 (Tsien, Ann. Rev. Biophys. Bioeng. 12, 91-116), which shows a Ca-dependent absorbance change at visible wavelengths, to record Ca transients in frog twitch fibers at 16°C. After micro-injection into the myoplasmic space, the resting spectrum of the dye was closely similar to the in vitro calibration in a zero Ca solution, while the peak amplitude of the Ca-dye signal following a single action potential had the wavelength dependence of the Ca-dye difference spectrum. Moreover, no evidence was detected for the existence of a dye-related dichroic signal. However, as judged from comparisons with the intrinsic birefringence signal used as a temporal bench mark, the time course of the Azo1 signal is probably slower than that recorded with Ap III. Thus Azo1 appears able to track myoplasmic Ca transients in a relatively simple fashion but with a delay having a time constant of possibly 3-4 msec. Calibration of the Ca-dye signal, using the measured Ca-Azo1 dissociation constant of 3.7 μM (140 mM-KCl, pH 6.90, 22°C) indicates that free Ca in a highly stretched fiber probably does not rise much above 1 μM following a single action potential.

Supported by MDA and NIH grant NS 17620.

W-AM-H9 EFFECT OF ALCOHOLS ON BIREFRINGENCE, CALCIUM AND TENSION TRANSIENTS IN FROG SKELETAL MUSCLE FIBERS. P. C. Pape and S. M. Baylor, Dept of Physiology, University of Pennsylvania.

Experiments were carried out to examine the effect of alcohols on E-C coupling. Intact single fibers were mounted at long sarcomere spacing in a normal Ringer's solution (15-17°C) and activated by action potential stimulation. Changes in the intrinsic birefringence signal were used as an indication of changes in E-C coupling. The effect of 1% ethanol (170 mM) was to increase the amplitude (by 10-20%) and time-to-peak (by 5-15%) of the birefringence signal, without affecting the initial rising phase of the signal. A single experiment done following injection of the Ca-indicator dye Azo1 (see related abstract) showed a similar potentiating effect of ethanol (200 mM) on both the myoplasmic free Ca transient and the birefringence signal. Experiments using the voltage-sensitive dye WW375 indicate that the ethanol effect on the birefringence signal is not explained by a change in the action potential. As previously reported by Khan (Acta Physiol. Scand. 111, 425, 1981) the twitch tension response in 1% ethanol decreased in most experiments, although we occasionally observed a small increase. Methanol, up to at least 0.8 M, always decreased the tension response, without significantly affecting the birefringence signal. In contrast, propanol and butanol increased both the birefringence and tension responses, but at much lower concentrations than required with ethanol. These results suggest at least two different effects of alcohols on E-C coupling. One effect is to decrease the twitch response, perhaps via some direct interaction with the contractile proteins. The other is to increase the birefringence, calcium and twitch responses, apparently by some effect on membranes, as evidenced by the dependence on alcohol chain length. Possible sites of action include inhibition of the SR Ca pump or enhancement of SR Ca release due to a delay in some process involved in turning off Ca release.

Supported by NIH grant NS 17620.

W-AM-H10 EXTRACELLULAR Ca MODIFIES Ca RELEASE FROM THE SARCOPLASMIC RETICULUM (SR) IN SKELETAL MUSCLE FIBERS. Eduardo Rios, Enrico Stefani‡, Gustavo Brum and John Goldman, Department of Physiology, Rush Medical School, Chicago, and ‡Centro de Investigacion del IPN, Mexico.

Effects of external Ca (Ca_e) were observed in cut fibers of frog skeletal muscle under voltage clamp at 7°C. The time course of myoplasmic [Ca^{2+}] (Ca_i) was recorded with Antipyrylazo III. Voltage-dependent Ca flux into the myoplasm (influx + release from SR) was derived from the Ca_i records as described by Melzer et al. (Biophys. J. 45:637, 1984). Intramembrane charge movement was measured by conventional methods. Surface and T-tubule membrane Ca currents (I_{Ca}) were evaluated by direct substraction of total current in 0 Ca_e from total current in Ca-containing solutions. Results: 1. The time course of Ca_i is strongly dependent on Ca_e (see figure). The initial fast rising phase is independent of Ca_e. In 2 mM Ca_e this phase is followed by a prolonged increase in Ca_i; in 0 Ca_e by a decrease. 2. The prolonged increase is higher in higher Ca_e. 3. The effect of high Ca_e is reversed by 3 mM Cd. 4. I_{Ca} is ~ 30 nA in 2 mM Ca_e, corresponding to a Ca influx of 0.075 µM/ms. 5. Voltage-dependent Ca flux into the myoplasm is ~ 1 µM/ms larger in 2 mM Ca_e. Conclusions: extra Ca enters the myoplasm when a fiber is depolarized in a Ca-containing medium; most of it does not come from the outside as I_{Ca} but is probably an extra release from the SR. External Ca modulates Ca release. Supported by NIH and ‡CONICyT (Mexico).

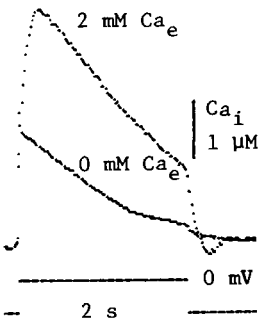

W-AM-H11 THE EFFECT OF EXTRACELLULAR Ca^{2+} AND STIMULATION RATE ON INTRACELLULAR Ca^{2+} AND TENSION IN RAT VENTRICULAR MUSCLE. C.H.Orchard and E.G.Lakatta, NIH, Baltimore, Md.

The amount of tension developed by rat heart muscle is greatly influenced by stimulation rate when perfusate [Ca^{2+}] (Ca_o) is below 3-4 mM. Unlike most other species, however, an increase in stimulation rate leads to a decrease in developed tension. When Ca_o is higher than 3-4 mM, changing stimulation rate has little effect on developed tension. We have investigated, therefore, whether: i) the negative force-frequency relationship observed at low Ca_o is due to changes in the amount of Ca^{2+} entering the myoplasm to initiate contraction. ii) the flat force-frequency relationship observed at high Ca_o is because the amount of Ca^{2+} initiating contraction does not change, or whether other factors are limiting the amount of tension developed.

The photoprotein aequorin was micro-injected into superficial cells of rat papillary muscles. Tension and aequorin light (a function of intracellular [Ca^{2+}]) were monitored. At 2 mM Ca_o, increasing stimulation frequency from 0.33 to 0.66 Hz significantly ($P < 0.05$) decreased peak tension and the peak of the aequorin light transient, to 68±4 and 68±5% of control values respectively (mean ± S.E.M., n=6). Decreasing stimulation frequency from 0.33 to 0.2 Hz significantly ($P < 0.05$) increased both peak tension and peak light, to 114±6 and 126±9% of control respectively. At 8 mM Ca_o, changing stimulation frequency had no significant effect on peak tension or peak aequorin light. These results suggest that under these conditions developed tension is limited by the amount of Ca^{2+} entering the myoplasm to initiate contraction.

W-AM-H12 RELATIONSHIP BETWEEN FORCE AND INTRACELLULAR [Ca^{2+}] IN TETANIZED VENTRICULAR MYOCARDIUM D.T. Yue+, E. Marban+, W.G. Wier, Dept. of Physiology, University of Maryland at Baltimore, and +The Johns Hopkins University, Baltimore, MD.

Determination of the steady-state relation between intracellular [Ca^{2+}] (Ca_i) and force in intact cardiac muscle would provide crucial information on the physiological control of force generation. Therefore, we measured steady force and Ca_i simultaneously in tetanized ferret papillary muscles. To measure Ca_i, we injected the Ca^{2+}-sensititive photoprotein aequorin into 40-100 cells of each muscle. Brief stimulation of muscles at 10 Hz in 5uM ryanodine at 30°C produced steady force (tetanus) and steady Ca_i (Fig. 1). Maximal Ca_i-activated force (5.67 g/mm^2, n=7) was clearly achieved in elevated extracellular [Ca^{2+}]. At lower levels of activation, very small 10 Hz oscillations of force and Ca_i were sometimes evident. In such cases, mean levels of Ca_i and force were obtained by filtering at 5Hz. Plots of steady-state force versus Ca_i (Fig. 2) were far steeper and shifted to the left (Hill coefficient = 5.94; Ca_i at half-maximal force = 0.50 uM; n=7) compared to those previously measured in skinned or hyperpermeable muscle. Thus the relation cannot be explained solely in terms of the Ca^{2+}-binding properties of the myofilaments.